In Cooperation with the Southern Nevada Water Authority (SNWA)

Geophysical Data from Spring Valley to Delamar Valley, East-Central Nevada

By Edward A. Mankinen, Carter W. Roberts, Edwin H. McKee, Bruce A. Chuchel, and Robert L. Morin

Open File Report 2007-1190

2007

U.S. Department of the Interior
U.S. Geological Survey

U.S. Department of the Interior
DIRK KEMPTHORNE, Secretary

U.S. Geological Survey
Mark D. Myers, Director

U.S. Geological Survey, Reston, Virginia 2007

For product and ordering information:
World Wide Web: http://www.usgs.gov/pubprod
Telephone: 1-888-ASK-USGS

For more information on the USGS—the Federal source for science about the Earth,
its natural and living resources, natural hazards, and the environment:
World Wide Web: http://www.usgs.gov
Telephone: 1-888-ASK-USGS

Suggested citation:
Mankinen, Edward A., Roberts, Carter W., McKee, Edwin H., Chuchel, Bruce A., and Morin, Robert L., 2007, Geophysical data from Spring Valley to Delamar Valley, east-central Nevada: U.S. Geological Survey Open File Report 2007-1190 [http://pubs.usgs.gov/of/2007/1190/]

Contents

Figures

Tables

Geophysical Data from Spring Valley to Delamar Valley, East-Central Nevada

By Edward A. Mankinen, Carter W. Roberts, Edwin H. McKee, Bruce A. Chuchel, and Robert L. Morin[1]

Abstract

Cenozoic basins in eastern Nevada and western Utah constitute major ground-water recharge areas in the eastern part of the Great Basin and these were investigated to characterize the geologic framework of the region. Prior to these investigations, regional gravity coverage was variable over the region, adequate in some areas and very sparse in others. Cooperative studies described herein have established 1,447 new gravity stations in the region, providing a detailed description of density variations in the middle to upper crust. All previously available gravity data for the study area were evaluated to determine their reliability, prior to combining with our recent results and calculating an up-to-date isostatic residual gravity map of the area. A gravity inversion method was used to calculate depths to pre-Cenozoic basement rock and estimates of maximum alluvial/volcanic fill in the major valleys of the study area. The enhanced gravity coverage and the incorporation of lithologic information from several deep oil and gas wells yields a much improved view of subsurface shapes of these basins and provides insights useful for the development of hydrogeologic models for the region.

[1] USGS, 345 Middlefield Road, Menlo Park, CA 94025

Introduction

The arid southwestern United States historically has been sparsely populated but the construction of dams, aqueducts, and pumping of groundwater allowed the relatively recent growth of major population centers throughout the region, with Nevada being one of the fastest-growing states in the Union. Increased demands on existing supplies have focused attention on finding new, alternative sources of water such as in the Great Basin regional aquifer system, a vast spring and ground-water system described by Harrill and Prudic (1998). Particular attention is being paid to the eastern part of the Great Basin where a major aquifer system is developed in a regionally-extensive, thick stratigraphic sequence of Paleozoic carbonate rocks (e.g., Welch and Bright, 2007). A second important ground-water system occurs in the Cenozoic basin-fill deposits found throughout the region. The current study is a continuation of a cooperative effort between the U.S. Geological Survey (USGS) and the Southern Nevada Water Authority (SNWA) to characterize the geophysical framework of several of these Cenozoic basins in eastern Nevada and western Utah (fig. 1; herein referred to as the study area). Gravity and magnetic data are described by Scheirer (2005) and Mankinen and others (2006, and this report), while data from concurrent audiomagnetotelluric (AMT) studies are described separately by McPhee and others (2006, 2007). Results of these studies are significantly increasing our understanding of the formation and subsurface shapes of the basins in this region and providing insights into the structures that may impede or allow ground-water flow.

Geologic Setting

Major extensional faulting began throughout the region at about 17 Ma (McKee, 1971; Christiansen and McKee, 1978; Stewart, 1978) and formed the horst-graben terrain that is typical of the Basin and Range Province. The study area (figure 1) is characterized by north-south, elongate mountain ranges and broad, flat alluvial-filled valleys. Valley floors are between 1,700 m and 1,800 m above sea level near the north end of the study area, decreasing to about 1,400 m toward the south. Most of the valleys are internally drained and contain playas. Crests of the major ranges average between about 1,700 m and 2,700 m above sea level. The highest summit in the region is Wheeler Peak in the Snake Range at 3,981 m above sea level. Geologic summaries covering much of the area can be found in Tschanz and Pampeyan (1970) and Hose and others (1976).

The oldest rocks in the region belong to the Precambrian McCoy Creek Group. The most abundant rock type in this group is massive quartzite, and similar rocks extend stratigraphically upward to include the Lower Cambrian Prospect Mountain Quartzite. Where not greatly faulted and fractured, these rocks form effective barriers to ground-water flow especially where they are in contact with younger carbonate rocks, and they may form the base of the carbonate-rock aquifer in areas where circulation extends throughout the entire stratigraphic thickness (Plume, 1996; Harrill and Prudic, 1998). These carbonate rocks range in age from the Middle Cambrian to Lower Triassic (Hose and others, 1976; Plume, 1996). The total stratigraphic thickness of the carbonate sequence ranges from about 1.5 km to as much as 9 km, and the composite unit is present throughout much of the eastern two-thirds of the Great Basin (Plume, 1996).

The youngest of the deep-water carbonate strata in the eastern Great Basin were deposited during Lower Triassic time, after which the continental margin shifted westward and the shallow sea retreated (e.g., Speed, 1978). The eastern Great Basin was uplifted, and erosion and continental deposition occurred locally during the remainder of Mesozoic time. No sedimentary rocks dating to this interval of time are known in the study area (fig. 1) with the possible exception of some small areas of tectonic breccia (Hose and others, 1976). Other rocks forming part of the pre-Cenozoic basement in the study area are a series of intrusive igneous rocks exposed along the southern Snake Range extending northward into the Kern Mountains (Hose and others, 1976; Best and others, 1974) and in the Deep Creek Range in Utah (Miller and others, 1999). Plutons likely exist beneath all calderas and many have been inferred throughout the region from interpretations of geophysical anomalies (Grauch and others, 1988; Ponce, 1990). Although plutons of the region range from Jurassic to Tertiary in age, all are grouped with the basement rocks because their density is similar to most of the pre-Cenozoic rocks, differing strongly from those of later eruptive and basin-fill rocks. Intrusive igneous rocks typically are barriers to ground-water flow (Plume, 1996) except in areas where extensively fractured.

The oldest Cenozoic sedimentary rocks in the study area are local occurrences in the central and northern Schell Creek Range (Hose and others, 1976). These are likely Eocene in age and pre-date the late Eocene to late Miocene calc-alkaline volcanic rocks found in many places in the area. A major volcanic episode began during the early Oligocene when voluminous ash-flow eruptions resulted in the formation of collapse caldera complexes throughout the Great Basin (e.g., Best and others, 1989). Although impermeable in hand sample, these densely-welded tuffs are easily fractured and can allow water circulation and may be major aquifers where continuous over large areas. Because many of the volcanic rocks in the study area occur as discontinuous outcrops on older rocks (Gans and others, 1989) except in the vicinity of the Caliente and Indian Peak caldera complexes (Ekren and others, 1977; Best and others, 1989), they have limited importance as regional aquifers.

Alluvial fill within the basins may range from a few hundred meters to several kilometers thick. This basin fill consists of clastic material derived from adjacent mountain ranges and is characterized by semi-consolidated to unconsolidated sand, gravel, silt, clay, and local evaporites with some interbedded volcanic units in many areas. The sand and gravel deposits form a major, shallow aquifer in the region where they are not clogged by clay or zeolitic intergranular materials. These aquifers are commonly exploited because groundwater in the valleys typically is within a few meters or tens of meters below the ground surface and easily reached by wells. Some of these basin-fill aquifers are hydraulically isolated from similar aquifers in adjacent valleys, while others are hydraulically connected by flow through the underlying carbonate aquifer (Plume, 1996).

Procedures

Gravity data were obtained using LaCoste and Romberg meters (G17C and G8N) and observed gravity values were referenced to two base stations. The base station at the Ely, Nevada airport (***ELYA***), at 39°17.59'N, -114°50.52'W, is tied to the International Gravity Standardization Net 1971 (ISGN 71) gravity datum (Morelli, 1974) and has an observed gravity value of 979,480.08 mGal. The second base (***ELYW***) is at a U.S. Coast and Geodetic Survey vertical angle benchmark stamped 'Ely West Base 1944.' This station is approximately 35 km southeast of Ely at 39°01.55'N, -114°34.71'W, and has an observed gravity value of 979,462.96 mGal (D. Ponce, USGS, written communication, 1991). Locations of gravity stations were determined using a differential GPS system with corrections provided by Continually Operated Reference Station (CORS) satellites. Locations after post-acquisition processing are accurate to within 1 meter, both horizontally and vertically.

Magnetic data were obtained from two areas in Spring Valley using a portable cesium-vapor magnetometer integrated with a differential GPS receiver. The magnetometer was mounted on a non-magnetic aluminum frame and towed behind a vehicle at speeds up to 40 mph. Measurements were taken at a rate of 10/second. The truck-towed magnetometer (TOM) system was designed and developed by R.L. Morin, D.A. Ponce, and J.M.G. Glen, USGS, in 2004. Because of the short duration of the traverses, we did not employ a stationary base-station magnetometer to record diurnal variations. Accuracy of the GPS readings is approximately 1 meter horizontally, and 5 meters vertically (J.E. Tilden, USGS, written communication, 2004).

Gravity Data

Since the initiation of the USGS-SNWA cooperative studies, 1,447 new gravity stations have been added between northern Spring and Tippet Valleys southward into Delamar Valley (fig. 2), including 434 from the current study (table 1). Locations of the gravity stations were designed both to improve regional gravity coverage and to provide high resolution gravity along selected traverses in the study area, particularly along some of the AMT lines established by McPhee and others (2006, 2007). Observed gravity at each station was adjusted by assuming a time-dependent linear drift between readings of a base station at the start and finish of each daily survey. This adjustment compensates for drift in the instrument's spring. Observed gravity values are considered accurate to about 0.05 mGal based on repeat measurements over several mountain calibration loops (Barnes and others, 1969; Ponce and Oliver, 1981).

Gravity data were reduced using standard gravity corrections (Blakely, 1995) and a reduction density of 2670 kg/m^3. Field terrain corrections (zones A and B of Hayford and Bowie, 1912) were carried out to 68 m using templates and charts (e.g., Plouff, 2000). Inner-zone terrain corrections for zones C and D (Hayford and Bowie, 1912), which are necessary to account for variations in topography near a gravity station, were obtained to a radial distance of 2 km using digitized topography in a digital elevation model (DEM) (D. Plouff, USGS, written communication, 2006). Outer terrain corrections, from 2 km to 167 km, are also calculated using digitized topography and a procedure by Plouff (1977). The resulting gravity anomaly is termed the complete Bouguer anomaly. A regional isostatic field was calculated using an Airy-Heiskanen (Heiskanen and Vening Meinesz, 1958) model for local compensation of topographic loads (Jachens and Roberts, 1981; Simpson and others, 1986). This model assumes a nominal crustal thickness of 25 km, a crustal density of 2670 kg/m^3, and a 400 kg/m^3 density contrast between the crust and mantle. This regional isostatic field was subtracted from the complete Bouguer anomaly, thus removing long-wavelength variations in the gravity field that are inversely related to topography. The resulting isostatic residual gravity anomaly, therefore, is a reflection of local density distributions within middle to upper crustal levels.

Gravity data obtained during the current study, and their associated parameters, are given in table 1 and are available via download as an Excel spreadsheet. Other gravity data available for the study area are from Ponce (1997), Scheirer (2005), Mankinen and others (2006), and unpublished data obtained by the USGS for the BARCAS (Basin and Range Carbonate Aquifer Study) Project (Sweetkind and others, 2007; Watt, and Ponce, 2007). Because prior gravity data for the study area were made by many different observers at different times, we examined the composite data set to remove duplicate and inconsistent entries. To test for possible errors, we first compared reported station elevations with elevations interpolated from 10- and 30-meter DEMs using a procedure by D. Plouff (USGS, written communication, 2005). Large elevation differences indicate possible errors in station location or elevation, and each station identified was examined individually to confirm the discrepancy. Some of these errors occurred because of imprecise locations (i.e., lack of significant digits in published reports) and were corrected with a high degree of confidence. If the source of the discrepancy could not be determined and corrected, the station was omitted from the data set. Observations from the revised data set were then gridded at a spacing of 0.5 km using the minimum curvature algorithm of Webring (1981), and the resulting isostatic residual gravity field (fig. 3) is considered reliable for subsequent analyses.

Gravity lineaments

We further analyze the gravity field to isolate lateral density boundaries of mid-crustal sources. Cenozoic tectonic activity may be accommodated along these deep-seated structures and thus their identification can help locate subsurface faults controlling regional ground-water flow. The gravity anomalies in figure 3 were first analytically upward-continued by 3 km (Hildenbrand, 1983) to de-emphasize surface and near-surface features and enhance the contribution of deeper sources. Next, horizontal gradients were calculated (e.g., Cordell, 1979; Blakely, 1995) for the upward-continued gravity anomalies shown in figure 4a. When calculated for two-dimensional data grids, horizontal gradients will place narrow ridges over significant changes in density. The method of Blakely and Simpson (1986) was used to calculate maximum values of these gradients, the locations of which tend to overlie the edges of causative bodies that have abrupt, near-vertical contacts. The maxima in the long-wavelength gravity data, along with a visual inspection of the gradient "ridges" containing them, were used to define major gravity lineaments (figure 4b).

Gravity Inversion

To first order, the isostatic residual gravity field (fig. 3) reflects the pronounced contrast between dense (~2670 kg/m3) pre-Cenozoic basement rocks and the significantly less dense (generally < 2500 kg/m3) overlying volcanic and sedimentary basin-fill. Because of this relationship, the gravity inversion method of Jachens and Moring (1990) can be used to separate the isostatic residual anomaly into pre-Cenozoic "basement" and Cenozoic "basin" fields, thus allowing an estimate of thickness of Cenozoic alluvial fill within the area. The accuracy of thickness estimates derived by the gravity inversion technique depends on the assumed density-depth relation of the Cenozoic rocks and on the initial density assigned to the basement rocks.

Density of basement rocks is generally assumed to be 2670 kg/m3 and this value is considered appropriate in this area where major exposures consist of late Precambrian through late Paleozoic marine carbonate and quartzose sedimentary rocks. Subvolcanic Cenozoic intrusions are included here as part of the basement because their physical properties are similar to most of the older rocks, and differ greatly from those of the eruptive and basin-fill sedimentary sequences. The density of basin-filling deposits generally increases with the degree of compaction and consolidation, and thus usually correlates with depth of burial, as well as with other factors such as increasing water content. The density-versus-depth relationship we use (table 2) is the same used by Jachens and Moring (1990) and Saltus and Jachens (1995) to separate the isostatic residual anomaly into basement and basin fields, and similar to those shown to be widely applicable to other volcanic basin-fill deposits throughout Nevada (Blakely and others, 1998, 2000; Mankinen and others, 2003).

In the inversion process, the density of basement is allowed to vary horizontally but the density of basin-filling deposits is fixed using the functions in table 2. In this iterative approach, a first approximation of the basement gravity field is derived from gravity measurements made on exposed pre-Cenozoic rocks. This basement gravity field ignores the gravity effects of nearby basins and is subtracted from the observed gravity, which provides the first approximation of the basin gravity field. Using the selected density-depth relation, the thickness of the basin-filling deposits is then calculated. The gravitational effect of this first approximation of the basin-filling layer is computed at each known basement station. This effect is, in turn, subtracted from the first approximation of the basement gravity field, and the process is repeated until successive iterations produce no substantial changes in the basement gravity field.

A modified version of the inversion method used here (B.A. Chuchel, unpublished data, 2005) allows basement gravity values to be approximated by correcting the isostatic gravity anomaly at sites where depth to basement is known from deep boreholes (Garside and others, 1988; Hess, 2004) or inferred from seismic data (Gans and others, 1985). At locations where wells did not penetrate the full thickness of basin fill, the maximum depths reached were used as minimum constraints in the iterative process. Information on oil and gas wells for Nevada and Utah is available at http://www.nbmg.unr.edu/lists/oil/oil.htm and http://ogm.utah.gov/oilgas/, respectively, and all constraints used are shown in figure 5. Results of the inversion (figure 6) were gridded at a spacing of 2.0 km using a minimum curvature algorithm Webring (1981).

Aeromagnetic Data

Aeromagnetic surveys encompassing the study area were originally presented by Zietz and others (1976, 1978), Mabey and others (1978), and Hildenbrand and others (1983), and discussed in detail by Plume (1996). Because of widely disparate aeromagnetic survey specifications from many areas, all data from Canada, Mexico, and the United States were reprocessed and merged into a coherent representation of the data, and compiled as a new digital magnetic anomaly database and map for North America (North American Magnetic Anomaly Group (NAMAG), 2002). A subset of this latest compilation was extracted for the Spring and Snake Valleys area shown in figure 7. Flight-line spacing of the original aeromagnetic surveys within this area ranged from 1.6 to 8.0 km in Nevada (Zietz and others, 1978; Hildenbrand and others, 1988) and from 1.6 to 3.2 km in Utah (Zietz and others, 1976).

A number of relatively small, strong magnetic highs in the northern part of the study area are associated with mapped outcrops of volcanic rock (Gans and others, 1989; Hagstrum and Gans, 1989) and the continuation of the anomalies indicate that these rocks also are present and more extensive in the subsurface. Although one of the largest plutons in the region forms the core of the Kern Mountains, it is expressed by a weak magnetic anomaly (figure 7). The main intrusion in this composite pluton, the Tungstonia Granite of Best and others (1974) is atypical among Great Basin granitic plutons. It is a Cretaceous (~75 Ma, Lee and others, 1986), deeply weathered two-mica granite containing phenocrystic muscovite, abundant aplite dikes and aplitic borders, all probably contributing to its weak magnetic signature. Younger (~35 Ma) intrusions of the immediate area are more typical with the absence of muscovite and the presence of ubiquitous Fe-Ti oxides (Best and others, 1974), and thus are probably more magnetic.

Several outcrops of Mesozoic intrusive rocks occur in the Snake Range NW of Baker (Hose and Blake, 1970; Stewart and Carlson, 1978), and Grauch and others (1988) and Ponce (1990) consider the large positive magnetic anomaly in this area (figure 7) to represent a buried pluton(s) at depth. The more subdued anomalies NW of Baker within Spring Valley (figure 7) may also represent buried granitic plutons (Ponce, 1990).

Ground Magnetic Data

Ground magnetic traverses using the truck-towed magnetometer were conducted within two areas of Spring Valley (figure 8). The first, profile “Spring_E1,” was along Highway 50 east of Majors Place. This traverse was conducted because our previous investigation of Rattlesnake Knoll (aka Rattlesnake Heaven prospect) indicated that the volcanic breccia forming the knoll might be extensive in the subsurface (Mankinen and others, 2006). A drill hole located near the top of the knoll was also reported to have penetrated igneous rock at depth (G.L. Dixon, oral communication, 2006). The second traverse, profile “Spring_E2,” was designed to investigate one of the weak magnetic anomalies possibly representing a small pluton (Ponce, 1990). Ground magnetic traverses, “Spring_E1” and “Spring_E2,” are shown in figures 9 and 10, respectively. Aeromagnetic data along both traverses are also shown in these to figures to illustrate the improvement in delineating weak magnetic anomalies. The magnetic signal along traverse Spring_E1 (figure 9) indicates the possibility of two or more distinct magnetic sources, one of which seems to correspond with the gravity anomaly associated with the volcanic breccia. Only a single magnetic source is indicated by the Spring_E2 traverse (figure 10), and it has no gravity expression.

Depth-to-magnetic source

Although there are different methods to estimate depth to a magnetic source (Blakely, 1995), here we use the graphical method described by Peters (1949). This method is easy to apply and is based on the fact that the horizontal gradient of a magnetic anomaly is proportional to the depth of the source (i.e., the steeper the gradient, the shallower the source). Peters' method also assumes that the magnetic anomaly is caused by a two-dimensional body with vertical sides and a uniform, nearly vertical magnetization. These assumptions are not strictly applicable in many geologic situations, and the depth estimations should thus be considered as approximations. Peters' method assigns different proportionality constants depending on whether the causative body is “very thin,” “very thick,” or has an “intermediate thickness.” General practice is to assume a body of intermediate thickness (unspecified), and we use this assumption as a first approximation.

An inspection of the gradients of the main magnetic anomaly along the Spring_E1 traverse indicates that the source on the western end is considerably shallower than that on the eastern end. Peters' method provides an estimate of approximately 600 m to the top of the magnetic source on the west and nearly 1 km on the east. Estimated depths to the pre-Cenozoic basement surface (figure 6) beneath the magnetic anomaly along this traverse range from about 700 m on the west to 100 m on the east. It is possible that some of the magnetic source rocks at the western part of the traverse may be within the basin fill, whereas toward the east the source(s) are clearly within the basement. Because this eastern source is within the basement rocks, it most likely represents a buried pluton. If true, we assume that it is probably a “very thick” body and Peters’ method yields a revised estimate of approximately 800 m to the top of the body, still well below the basement surface in this area.

Applying Peters’ method to the magnetic anomaly along the Spring_E2 traverse yields an estimate of approximately 400 m to the top of the magnetic source. Estimated depths to the pre-Cenozoic basement surface (figure 6) directly beneath this magnetic anomaly are all approximately 900 m, indicating that the magnetic source rocks occur within the alluvial fill and are most likely volcanic in origin. If true, a depth calculation assuming a “very thin” body yields an estimate of 500 m to the top of the source, still well within the alluvial fill.

The only deep drill-holes in the vicinity of the Spring_E2 traverse are Bastian Creek No. 1 (figures 5 and 8) and Yelland No. 1 (figure 5). Bastian Creek No. 1 encountered igneous rock at a depth of 1.4 km, approximately 140 m below the basement surface at this locality. Yelland No. 1 encountered a sequence of volcanic rocks within the basin fill between 1.09-km and 1.47-km depth. Note that the igneous intrusion at the Bastian Creek well has no magnetic expression. Analyses of basement gravity anomalies show that a basement gravity low extends across the central part of the state (Blakely and Jachens, 1991; Ponce and Tilden, 2006; Watt and Ponce, 2007) perhaps reflecting concealed, relatively low density silicic intrusions over much of the region. Blakely (1988) shows that part of this area is characterized by a general absence of short wavelength magnetic anomalies that roughly corresponds to a belt of muscovite-bearing granitic rocks. Data from the Bastian Creek well, along with the lack of magnetic expression, is consistent with the presence of a non-magnetic, two-mica granite similar to the Kern Mountain pluton and supportive of the above speculations. Our depth calculations along the Spring_E2 traverse, along with well log information from the two drill holes, further indicate that the magnetic anomalies identified in central Spring Valley (figures 7 and 8) have volcanic rather than plutonic sources.

Conclusions

Gravity data collected during the course of these cooperative studies have allowed a much improved definition of basins in the region. Mankinen and others (2006) compared their depth-to-basement calculations for the Spring and Snake Valleys area with a previously published map (Saltus and Jachens, 1995), illustrating the importance of an improved data distribution and incorporation of drill-hole data not available for the earlier interpretation. Our latest depth-to-basement calculations (figure 6) for the study area shown in figure 1 are further refinements to those of Scheirer (2005) and Mankinen and others (2006). Identification of major gravity lineaments (figure 4b) will help in locating subsurface faults controlling regional ground-water flow. Many of these lineaments clearly reflect basin-bounding faults indicating typical Basin and Range horst-graben structure for the major basins of the study area. Also see locations of maxima in the horizontal gradient of the gravity field as calculated by Scheirer (2005). Results from measurements made with the truck-towed magnetometer show the potential for delineating and interpreting weak magnetic anomalies that are poorly expressed in existing aeromagnetic surveys of the region. Magnetometer data have been collected along some of the AMT profiles established by McPhee and others (2006, 2007) and will be processed in the future. Our cooperative studies are continuing and the immediate focus will be in the vicinity of potential well sites within Spring Valley.

Acknowledgements

This study was performed with the cooperation of the Southern Nevada Water Authority (SNWA) whose support is greatly appreciated. We also thank Bryce Johnson for assistance in the field. Reviews by J.M.G. Glen and D.S. Scheirer, and informal comments by G.L. Dixon, helped to clarify and improve the manuscript. Discussions with G.L. Dixon during the course of this study proved very helpful.

References Cited

Barnes, D.F., Oliver, H.W., and Robbins, S.L., 1969, Standardization of gravimeter calibrations in the Geological Survey: Eos, Transactions of the American Geophysical Union, v. 50, p. 526-527.

Best, M.G., Christiansen, E.H., and Blank, H.R., Jr., 1989, Oligocene calc-alkaline rocks of the Indian Peak volcanic field, Nevada and Utah: Geological Society of America Bulletin, v. 101, p. 1076-1090.

Best, M.G., Armstrong, R.L., Graustein, W.C., Embree, G.F., and Ahlborn, R.C., 1974, Mica granites of the Kern Mountains pluton, eastern White Pine county, Nevada: Remobilized basement of the Cordilleran miogeosyncline?: Geological Society of America Bulletin, v. 85, p. 1277-1286.

Best, M.G., Christiansen, E.H., Deino, A.L., Grommé, C.S., McKee, E.H., and Noble, D.C., 1989, Eocene through Miocene volcanism in the Great Basin of the western United States, *in* Chapen, C.E., and Zedik, V., eds., Field excursions to volcanic terranes in the western United States, v. II: Cascades and Intermountain west: New Mexico Bureau of Mines and Mineral Resources Memoir 47, p. 91-133.

Blakely, R.J., 1988, Curie temperature isotherm analysis and tectonic implications of aeromagnetic data from Nevada: Journal of Geophysical Research, v. 93, p. 11,817-11,832.

Blakely, R.J., 1995, *Potential Theory in Gravity and Magnetic Applications*: Cambridge University Press, 441 p.

Blakely, R.J., and Jachens, R.C., 1991, Regional study of mineral resources in Nevada: Insights from three-dimensional analysis of gravity and magnetic anomalies: Geological Society of America Bulletin, v. 103, p. 795-803.

Blakely, R.J., and Simpson, R.W. 1986, Approximating edges of source bodies from magnetic or gravity anomalies: Geophysics, v. 51, p. 1494-1498.

Blakely, R.J., Langenheim, V.E., Ponce, D.A., and Dixon, G.L., 2000, Aeromagnetic survey of the Amargosa Desert, Nevada and California: A tool for understanding near-surface geology and hydrology: U.S. Geological Survey Open-File Report 00-188, 35 p.

Blakely, R.J., Morin, R.L., McKee, E.H., Schmidt, K.M., Langenheim, V.E., and Dixon, G.L., 1998, Three-dimensional model of Paleozoic basement beneath Amargosa Desert and Pahrump Valley, California and Nevada: Implications for tectonic evolution and water-resources: U.S. Geological Survey Open-File Report 98-496, 27 p.

Christiansen, R.L., and McKee, E.H., 1978, Late Cenozoic volcanic and tectonic evolution of the Great Basin and Columbia Intermontane regions, *in* Smith, R.B., and Eaton, G.P., eds., Cenozoic tectonics and regional geophysics of the Western Cordillera: Geological Society of America Memoir 152, p. 283-311.

Cordell, L., 1979, Gravimetric expression of graben faulting in Santa Fe County and the Española Basin, *in* Ingersoll, R.V., ed., Guidebook to Santa Fe County, 30th Field Conference: New Mexico Geological Society, p. 59-64.

Ekren, E.B., Orkild, P.P., Sargent, K.A., and Dixon, G.L., Geologic map of Tertiary rocks, Lincoln County, Nevada: U.S. Geological Survey Miscellaneous Investigations Series Map I-1041, scale 1:250,000.

Gans, P.B., Mahood, G.A., and Schermer, E., 1989, Synextensional magmatism in the Basin and Range Province; A case study from the eastern Great Basin: Geological Society of America Special Paper 233, 53 p.

Gans, P.B., Miller, E.L., McCarthy, J., and Ouldcott, M.L., 1985, Tertiary extensional faulting and evolving ductile-brittle transition zones in the northern Snake Range and vicinity: New insights from seismic data: Geology, v. 13, p. 189-193.

Garside, L.J., Hess, R.H., Fleming, K.L., and Weimer, B.S., 1988, Oil and gas developments in Nevada: Nevada Bureau of Mines and Geology Bulletin 104 (on-line database, updated June, 2004).

Grauch, V.J.S., Blakely, R.J., Blank, H.R., Oliver, H.W., Plouff, D., and Ponce, D.A., 1988, Geophysical delineation of granitic plutons in Nevada: U.S. Geological Survey Open-File Report 88-11, scale 1:1,000,000.

Hagstrum, J.T., and Gans, P.B., 1989, Paleomagnetism of the Oligocene Kalamazoo Tuff: Implications for middle Tertiary extension in east central Nevada: Journal of Geophysical Research, v. 94, p. 1827-1842.

Harrill, J.R., and Prudic, D.E., 1998, Aquifer systems in the Great Basin region of Nevada, Utah, and adjacent states–Summary report: U.S. Geological Survey Professional Paper 1409–A,
66 p.

Hayford, J.F., and Bowie, William, 1912, The effect of topography and isostatic compensation upon the intensity of gravity: U.S Coast and Geodetic Survey Special Publication 10, 132 p.

Heiskanen, W.A., and Vening Meinesz, F.A., 1958, The Earth and its Gravity Field: New York, McGraw-Hill, 470 p.

Hess, R.H., 2004, Nevada oil and gas well database (NVOILWEL): Nevada Bureau of Mines and Geology Open-File Report 04-1, 288 p.

Hildenbrand, T.G., 1983, FFTFIL: A filtering program based on two-dimensional Fourier analysis: U.S. Geological Survey Open-File Report 83-237, 61 p.

Hildenbrand, T.G., Kucks, R.P., and Sweeney, R.E., 1983, Digital colored magnetic-anomaly map of the Basin and Range Province: U.S. Geological Survey Open-File Report 83-189, 11 p.

Hose, R.K., and Blake, M.C., Jr., 1970, Geologic map of White Pine County, Nevada: U.S. Geological Survey Open-File Report 70-1660, scale ~1:146,000.

Hose, R.K., Blake, M.C., Jr., and Smith, R.M., 1976, Geology and mineral resources of White Pine County, Nevada: Nevada Bureau of Mines and Geology Bulletin 85, 105 p.

Jachens, R.C., and Moring, B.C., 1990, Maps of the thickness of Cenozoic deposits and the isostatic residual gravity over basement for Nevada: U.S. Geological Survey Open-File Report 90-404, 15 p.

Jachens, R.C., and Roberts, C.W., 1981, Documentation of program, ISOCOMP, for computing isostatic residual gravity: U.S. Geological Survey Open-File Report 81-574, 26 p.

Lee, D.E., Stacey, J.S.D., and Fisher, L., 1986, Muscovite-phenocrystic two-mica granites of NE Nevada are Late Cretaceous in age, *in* Shorter Contributions to Isotope Research: U.S. Geological Survey Bulletin 1622, p. 31-39.

Mabey, D.R., Zietz, I., Eaton, G.P., and Kleinkopf, M.D., 1978, Regional magnetic patterns in part of the Cordillera in the western United States, *in* Smith, R.B., and Eaton, G.P., editors, Cenozoic Tectonics and Regional Geophysics of the Western Cordillera: Geological Society of America Memoir 152, p. 93-105.

Mankinen, E.A., Hildenbrand, T.G., Fridrich, C.J., McKee, E.H., and Schenkel, C.J., 2003, Geophysical setting of the Pahute Mesa–Oasis Valley region, southern Nevada: Nevada Bureau Mines and Geology Report 50, CD-ROM, 45 p.

Mankinen, E.A., Roberts, C.W., McKee, E.H., Chuchel, B.A., and Moring, B.C., 2006, Geophysical Data from the Spring and Snake Valleys Area, Nevada and Utah: U.S. Geological Survey Open-File Report 2006-1160, 42 p.

McKee, E.H., 1971, Tertiary igneous chronology of the Great Basin of western United States–Implications for tectonic models: Geological Society of America Bulletin, v. 82, p. 3497-3502.

McPhee, D.K., Chuchel, B.A., and Pellerin, L., 2006, Audiomagnetotelluric data from Spring, Cave, and Coyote Spring Valleys, Nevada: U.S. Geological Survey Open-File Report 2006-1164, 41 p.

McPhee, D.K., Chuchel, B.A., and Pellerin, L., 2007, Audiomagnetotelluric data and 2D models from Spring, Snake, and Three Lakes Valleys, Nevada: U.S. Geological Survey Open-File Report 2007-1181, 94 p.

Miller, E.L., Dumitru, T.A., Brown, R.W., and Gans, P.B., 1999, Rapid Miocene slip on the Snake Range–Deep Creek Range fault system, east-central Nevada: Geological Society of America Bulletin, v. 111, p. 886-905.

Morelli, C., ed., 1974, The International Gravity Standardization Net 1971: International Association of Geodesy Special Publication 4, 194 p.

North American Magnetic Anomaly Group (NAMAG), 2002, Digital data grids for the magnetic anomaly map of North America: U.S. Geological Survey Open-File Report 02-414, 4 p.

Nichols, W.D., 2000, Regional ground-water evaporation and ground-water budgets, Great Basin, Nevada: U.S. Geological Survey Professional Paper 1628, 108 p.

Papke, K.G., 1979, Fluorspar in Nevada: Nevada Bureau of Mines and Geology Bulletin 93, 77 p.

Peters, L.J., 1949, The direct approach to magnetic interpretation and its practical application: Geophysics, v. 14, p. 290-320.

Plouff, Donald, 1977, Preliminary documentation for a FORTRAN program to compute gravity terrain corrections based on topography digitized on a geographic grid: U.S. Geological Survey Open-File Report 77-535, 45 p.

Plouff, Donald, 2000, Field estimates of gravity terrain corrections and Y2K-compatible method to convert from gravity readings with multiple base stations to tide- and long-term drift-corrected observations: U.S. Geological Survey Open-File Report 00-140, 37 p.

Plume, R.W., 1996, Hydrogeologic framework of the Great Basin region of Nevada, Utah and adjacent states: U.S. Geological Survey Professional Paper 1409–B, 64 p.

Ponce, D.A., 1990, Gravity and magnetic anomalies in the Ely quadrangle, Nevada, and anomalies related to granitic plutons, *in* Geology and Ore Deposits of the Great Basin: Reno, Geological Society of Nevada, p.103-106.

Ponce, D.A., 1997, Gravity data of Nevada: U.S. Geological Survey Digital Data Series DDS-42, CD-ROM, 27 p.

Ponce, D.A., and Oliver, H.W., 1981, Charleston Peak gravity calibration loop, Nevada: U.S. Geological Survey Open-File Report 81-985, 20 p.
Ponce, D.A., and Tilden, J.E., 2006, Basement gravity feature in east-central Nevada and west-central Utah and its tectonic implications: Eos Transactions of the American Geophysical Union, v. 87, no. 52, Supplement 26, Dec. 2006.
Saltus, R.W., and Jachens, R.C., 1995, Gravity and basin-depth maps of the Basin and Range Province, western United States: U.S. Geological Survey Geophysical Investigations Map
GP-1012, scale 1:2,500,000.
Scheirer, D.S., 2005, Gravity studies of Cave, Dry Lake, and Delamar Valleys, east-central Nevada: U.S. Geological Survey Open-File Report 2005-1339, 27 p.
Simpson, R.W., Jachens, R.C., Blakely, R.J., and Saltus, R.W., 1986, A new isostatic residual gravity map of the conterminous United States, with a discussion of the significance of the isostatic residual anomalies: Journal of Geophysical Research, v. 91, p. 8348-8372.
Speed, R.C., 1978, Paleogeographic and plate tectonic evolution of the early Mesozoic marine province of the western Great Basin, *in* Howell D.G., and McDougall, K.A., eds., Mesozoic paleogeography of the western United States: Los Angeles, Calif., Pacific Section, Society of Economic Paleontologists and Mineralogists, p.253-270.
Stewart, J.H., 1978, Basin-range structure in western North America: A review, *in* Smith, R.B., and Eaton, G.P., eds., Cenozoic tectonics and regional geophysics of the Western Cordillera: Geological Society of America Memoir 152, p. 1-31.
Stewart, J.H., and Carlson, J.E., 1978, Geologic Map of Nevada: U.S. Geological Survey, scale 1:500,000.
Sweetkind, D.S., Knochenmus, L., Ponce, D.A., Wallace, A., Scheirer, D., Watt, J.T., and Plume, R.W., 2007, Hydrogeologic framework, *in* Welch, A.H., and Bright, D.J., eds., Water resources of the Basin and Range carbonate-rock aquifer system, White Pine County, Nevada, and adjacent areas in Nevada and Utah–Draft report: U.S. Geological Survey Open-File Report 2007-1156 (in press).
Tschanz, C.M., and Pampeyan, E.H., 1970, Geology and mineral deposits of Lincoln County, Nevada: Nevada Bureau of Mines and Geology Bulletin 73, 188 p.
Watt, J.T., and Ponce, D.A., 2007, Geophysical framework investigations influencing ground-water resources in east-central Nevada and west-central Utah, with a section on Geologic and geophysical basin-by-basin descriptions by Wallace, A.R. , Watt, J.T., and Ponce, D.A.: U.S. Geological Survey Open-File Report 2007-1163, 40 p. 2 plates, scale 1:750,000.
Webring, M., 1981, MINC, –A gridding program based on minimum curvature: U.S. Geological Survey Open-File Report 81-1224, 43 p.
Welch, A.H., and Bright, D.J., editors, 2007, Water resources of the Basin and Range carbonate-rock aquifer system, White Pine County, Nevada, and adjacent areas in Nevada and Utah–Draft report: U.S. Geological Survey Open-File Report 2007-1156 (in press).
Zietz, I., Shuey, R., and Kirby, J.R., Jr., 1976, Aeromagnetic map of Utah: U.S. Geological Survey Geophysical Investigations Map GP-907, scale 1:1,000,000.
Zietz, I., Gilbert, F.P., and Kirby, J.R., Jr., 1978, Aeromagnetic map of Nevada: Color coded intensities: U.S. Geological Survey Geophysical Investigations Map GP-922, scale 1:1,000,000.

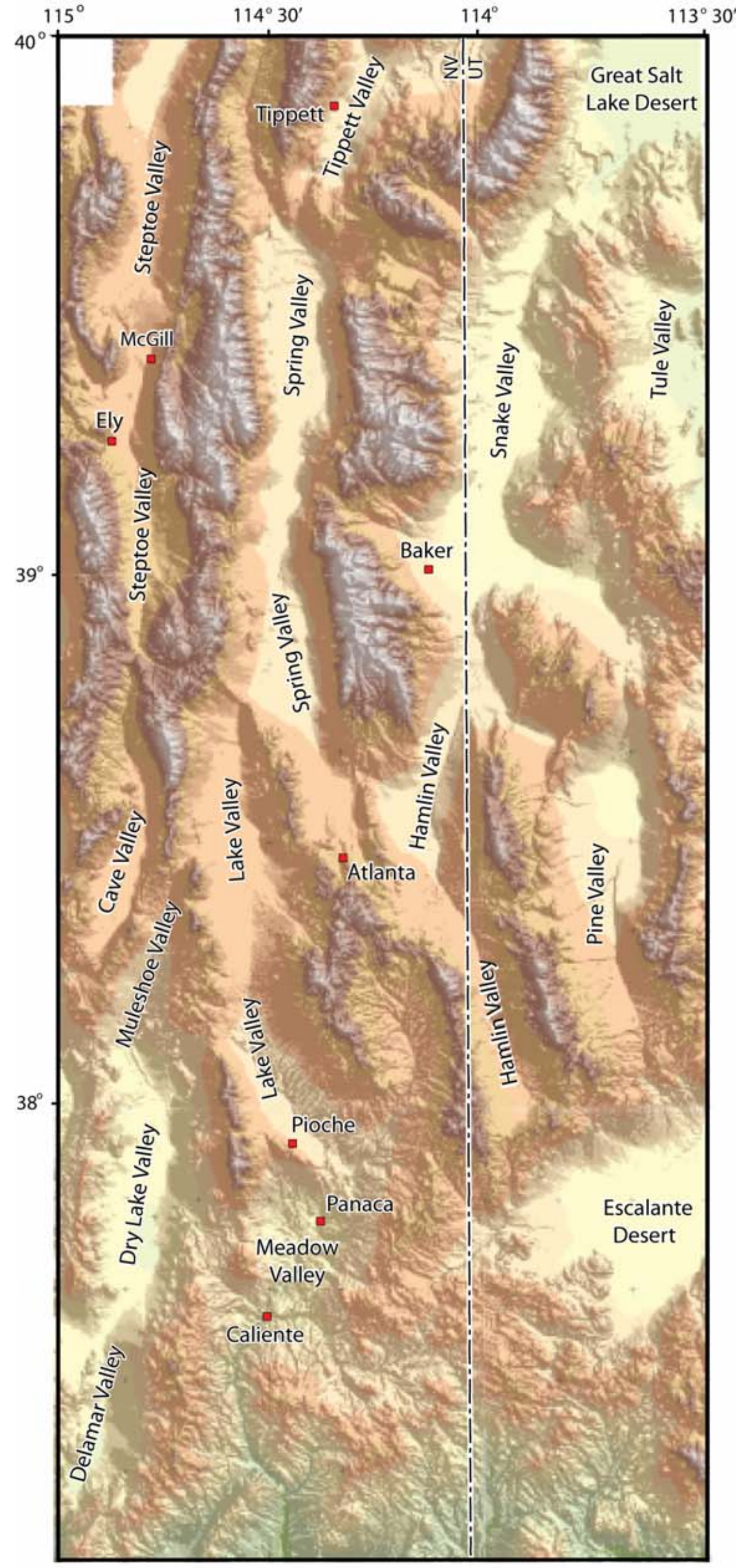

Figure 1. Shaded-relief map of the Spring Valley to Delamar Valley study area.

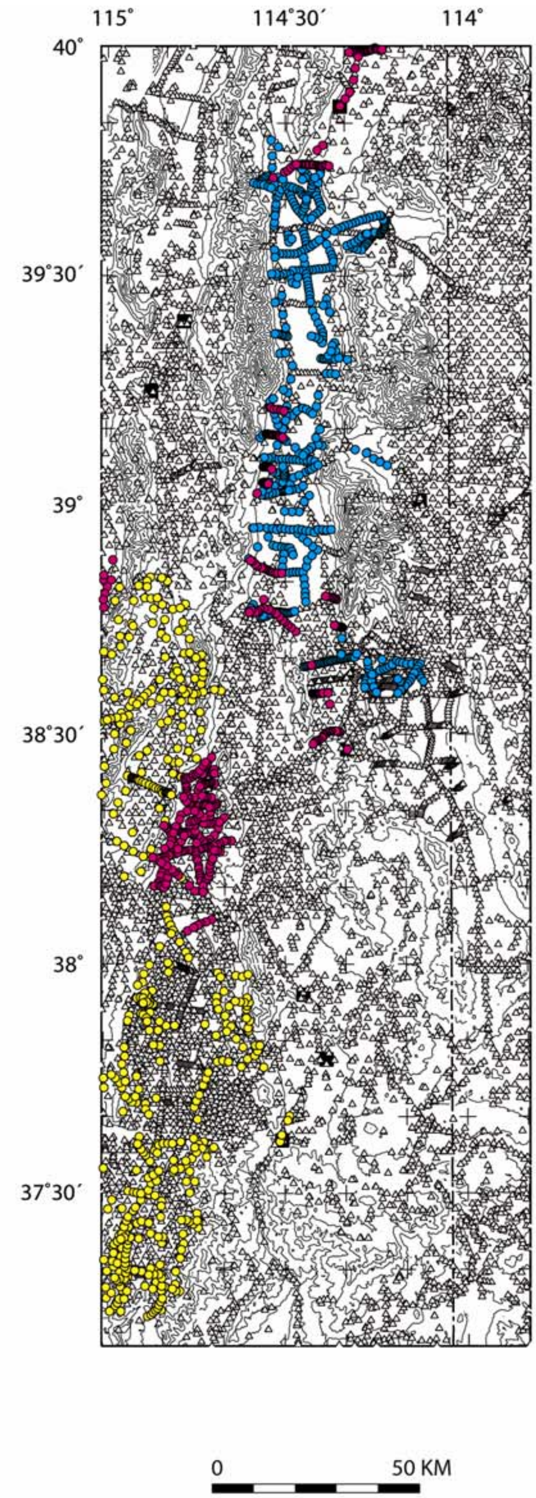

Figure 2. Locations of gravity stations in the study area. Triangles, previously available stations; Colored dots, stations added during the USGS-SNWA cooperative studies (○ = Scheirer, 2005; ● = Mankinen & others, 2006; ● = this study).

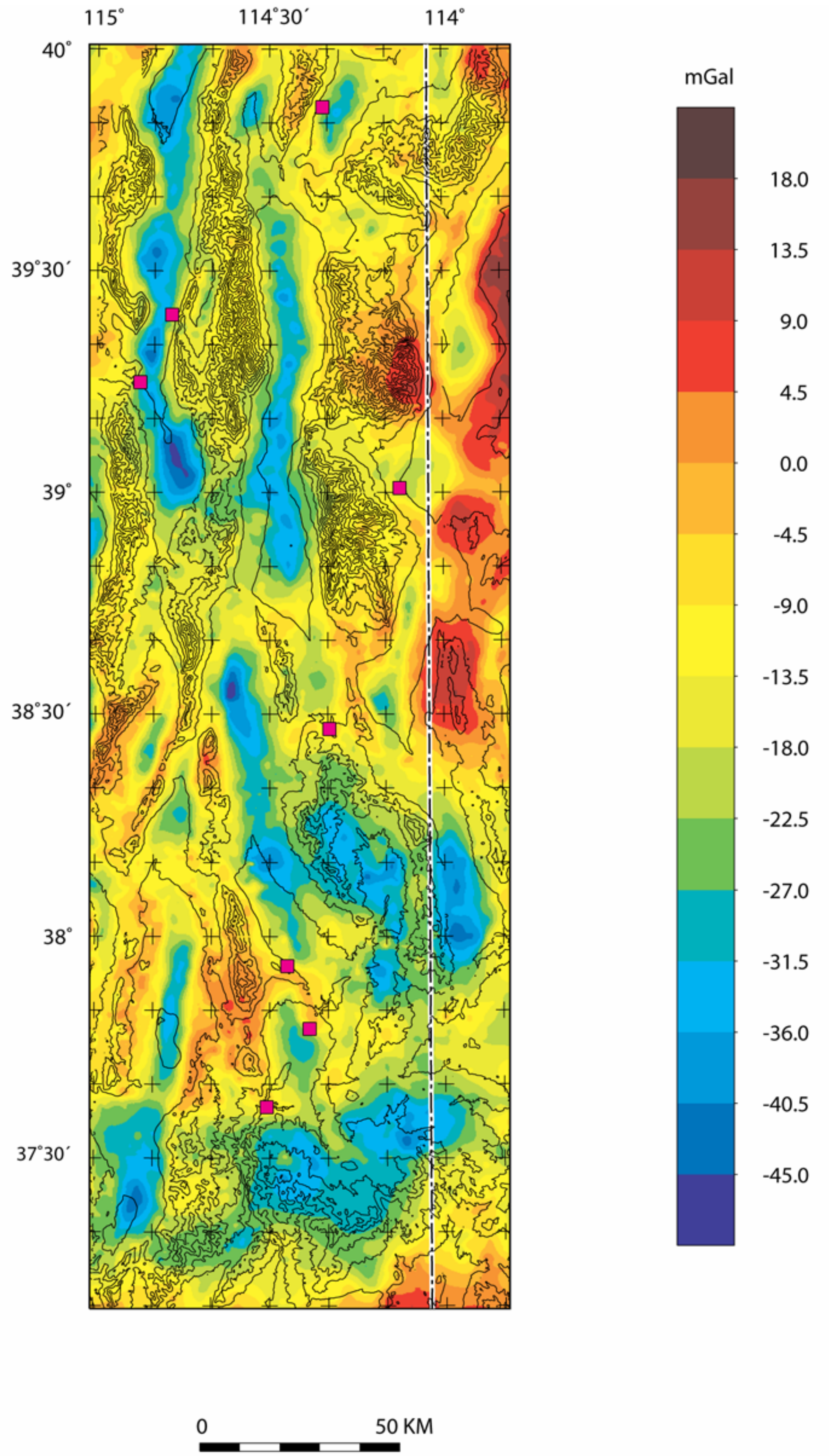

Figure 3. Isostatic gravity field. Anomalies reflect local density variations in the middle and upper crust.

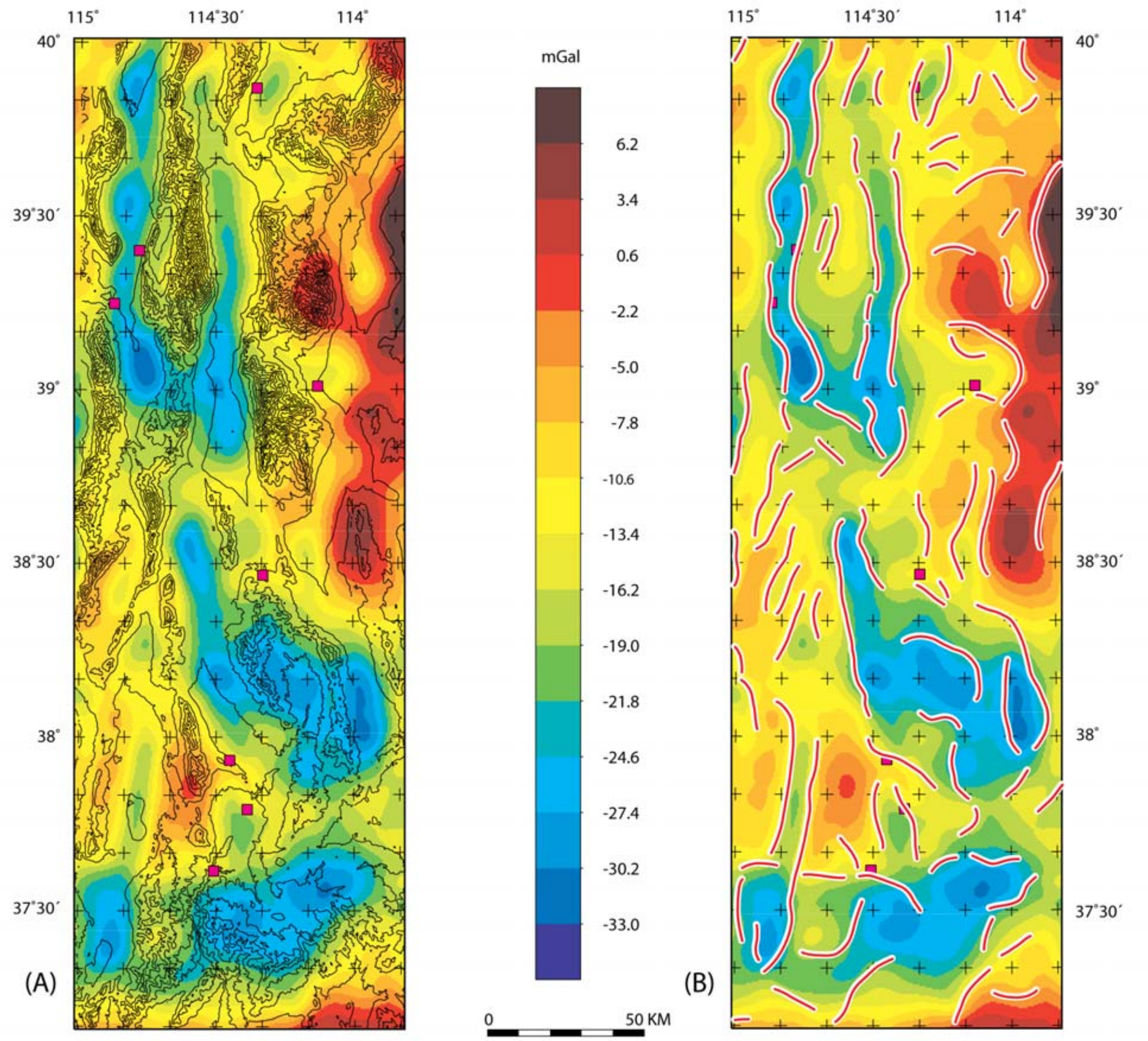

Figure 4. (A) Isostatic residual gravity anomalies upward continued 3 km to enhance deeper sources. (B) Same as (A), showing interpreted major gravity lineaments (see text).

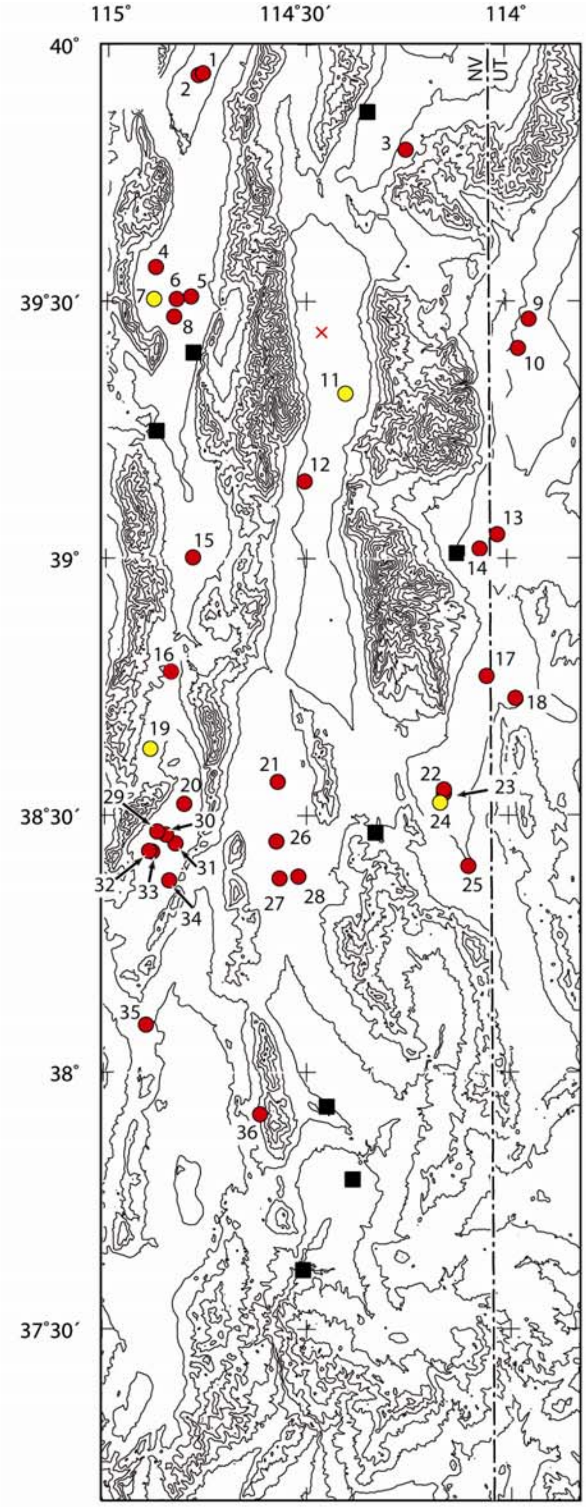

EXPLANATION

1. Steptoe Federal No. 17-14 (2.14 km)
2. Steptoe Unit No. 1 (2.09 km)
3. REMKIN Federal No. 1 (0.37 km)
4. Duck Creek No. 1 (2.44 km)
5. Nevada-Federal "A" No.1 (1.80 km)
6. Steptoe Federal 1-24 (1.63 km)
7. Grass Springs No. 1 (> 1.07 km)
8. Federal No. 54X-36 (1.71 km)
9. Cobra State 12-36 (0.99 km)
10. Mamba Federal 31-22 (0.87 km)
11. Yelland No. 1 (> 1.74 km)
12. Bastian Creek No. 1 (1.25 km)
13. Baker Creek Unit 1 (1.29 km)
14. Baker Creek No. 12-1 (1.41 km)
15. Titan Federal No. 1-9 (0.95 km)
16. Federal No. 1--Dwight M. Ross (1.46 km)
17. Outlaw Federal No. 1 (0.38 km)
18. Needle Anticline 1B (0.14 km)
19. Federal No. 1--Pease Willard (>1.91 km)
20. Foreland Federal No. 1-28 (1.02 km)
21. Saguaro Unit No. 1 (1.34 km)
22. Hamlin Wash No. 18-1 (0.93 km)
23. Hamlin Wash No. 19-1 (1.27 km)
24. Fletcher No. 1 (> 2.28 km)
25. Cobb Creek Federal No. 11-1 (0.11 km)
26. Dutch John Unit No. 1 (1.50 km)
27. Shogrin Federal No. 1 (1.33 km)
28. Apache/Frontier Exploration Federal No. 22-13 (0.53 km)
29. Cave MX (0.11 km)
30. Cave Valley Federal No. 13-10 (1.00 km)
31. Cave Valley Unit Federal No. 1 (2.02 km)
32. Flat Top Federal No. 27-16 (0.63 km)
33. Flat Top Federal No. 27-15 (0.55 km)
34. Sidehill Pass Federal No. 18-13 (1.55 km)
35. Dry Lake MX (0.10 km)
36. USA No. 1-30 (0.32 km)

Figure 5. Depth constraints (in parens) for the gravity inversion. Red dots, wells encountering pre-Cenozoic basement; Yellow dots, minimum depth constraints. Wells encountering basement at depths shallower than 100 meters not shown. Red X indicates maximum interpreted depth (~2.90 km) along the SOHIO seismic line (Gans & others, 1985).

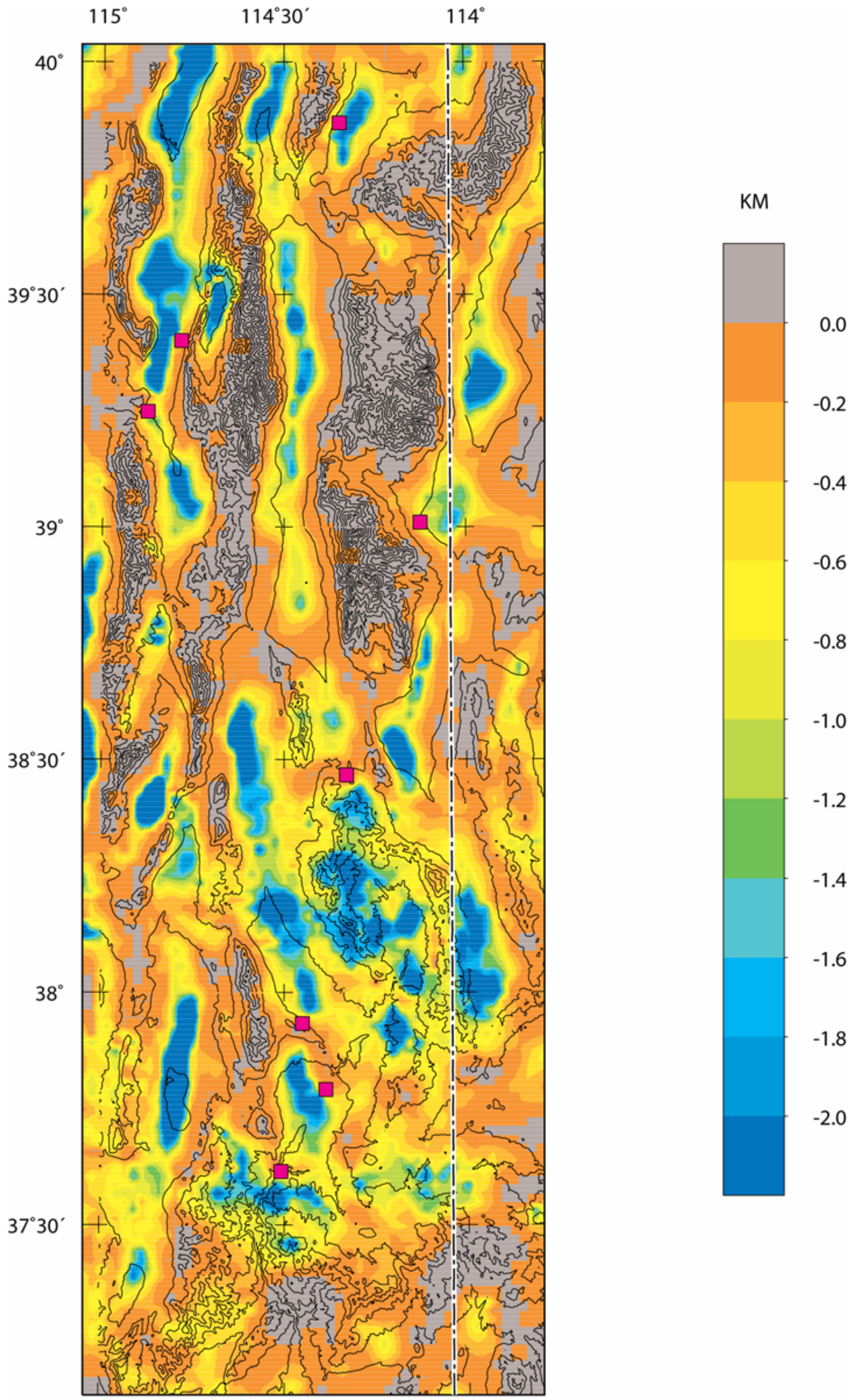

Figure 6. Depth to pre-Cenozoic basement calculated using gravity observations from the stations shown in figure 2 and the drill-hole constraints from figure 4.

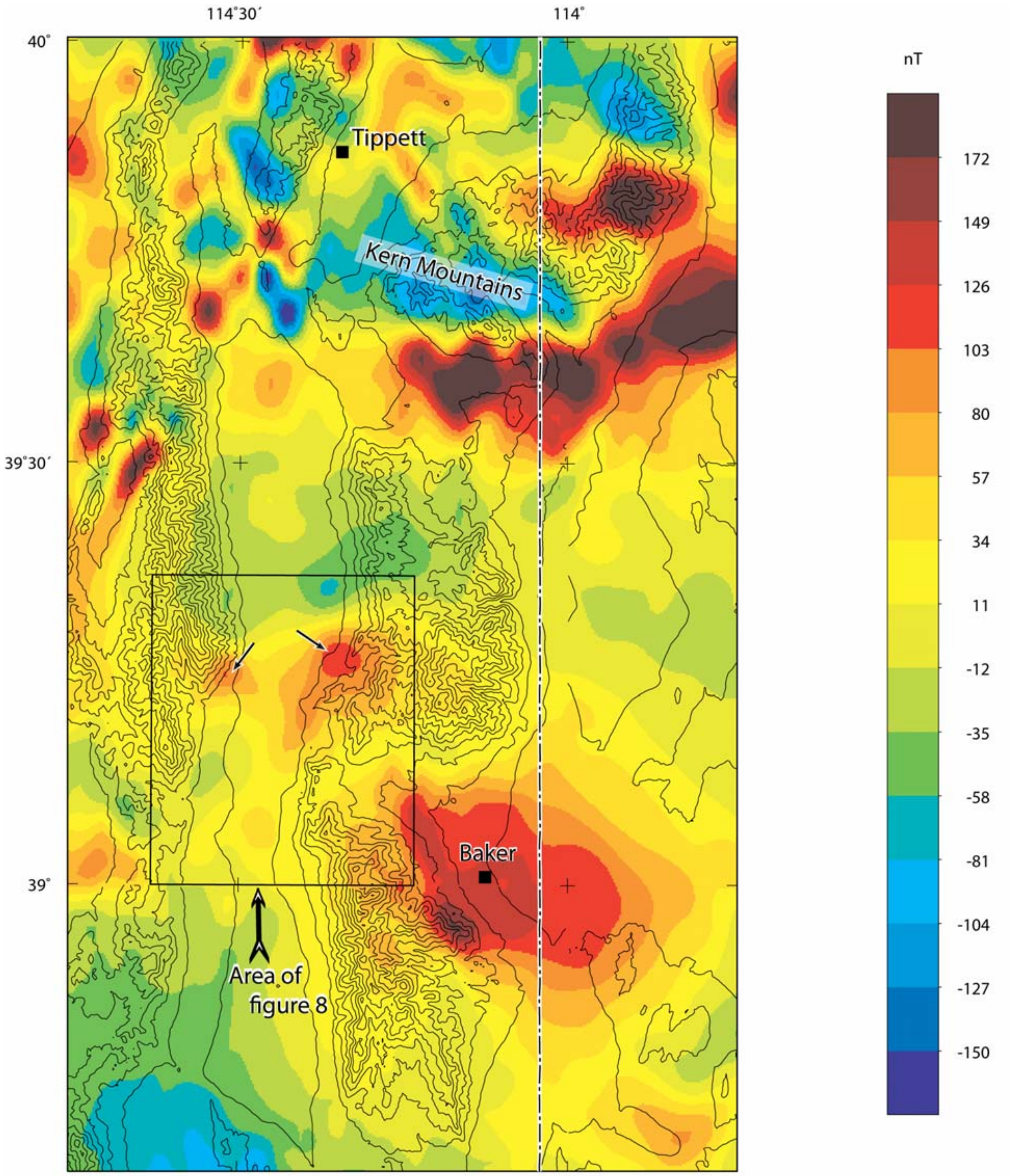

Figure 7. Aeromagnetic map of the Spring and Snake Valleys area, extracted from the digital magnetic anomaly database and map for North America (NAMAG, 2002). Colors represent measured magnetic field intensities relative to the International Geomagnetic Reference Field. Small arrows show locations of possible buried plutons (Ponce, 1990).

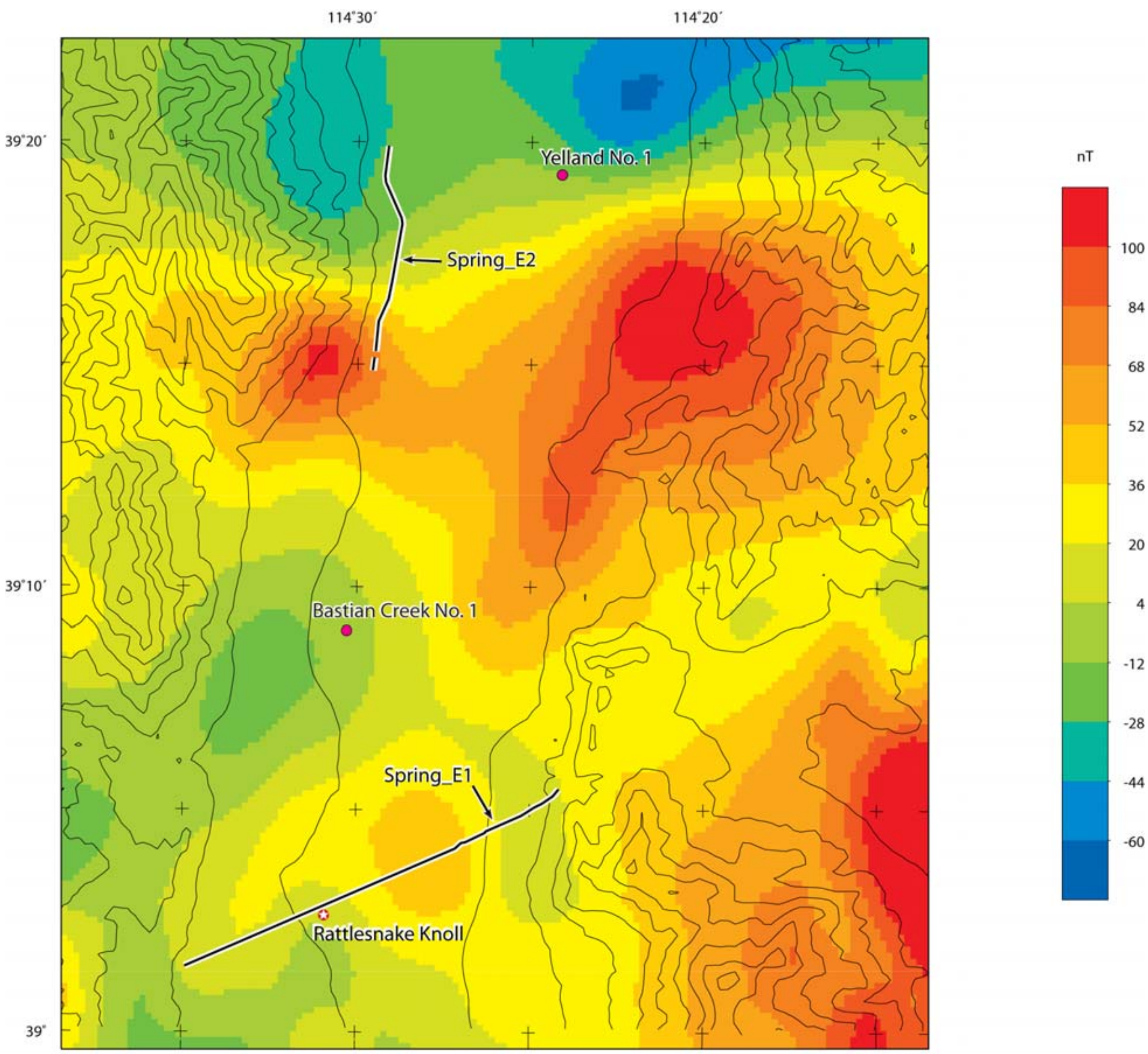

Figure 8. Aeromagnetic anomalies from figure 7 showing magnetic traverses conducted with the truck-towed magnetometer.

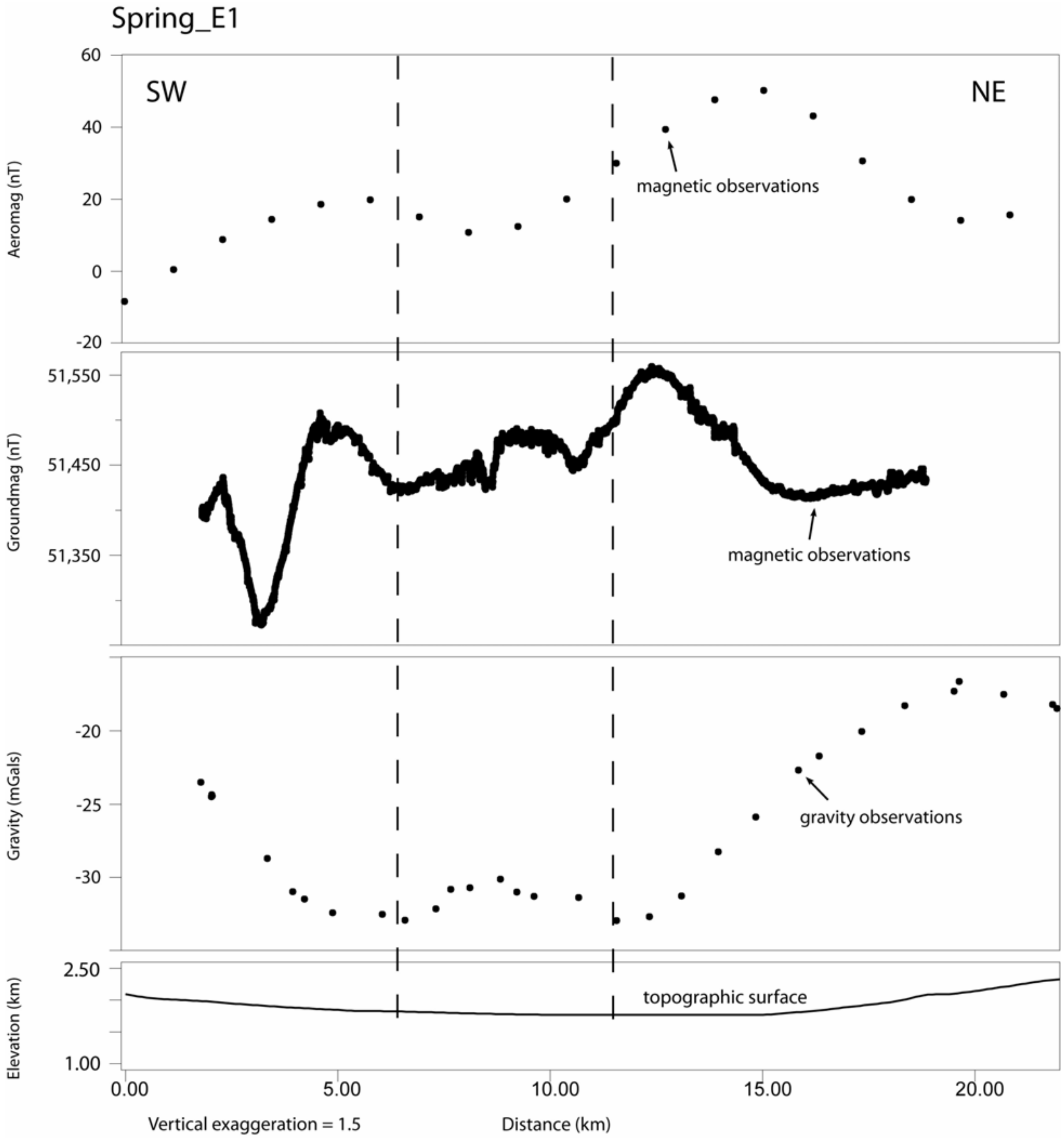

Figure 9. Ground magnetic traverse along line "Spring_E1." Upper panel shows aeromagnetic data from NAMAG (2002) for comparison. Vertical dashed lines show approximate limits of small gravity anomaly (see figure 8, Mankinen & others, 2006) associated with the exposed volcanic breccia at Rattlesnake Knoll.

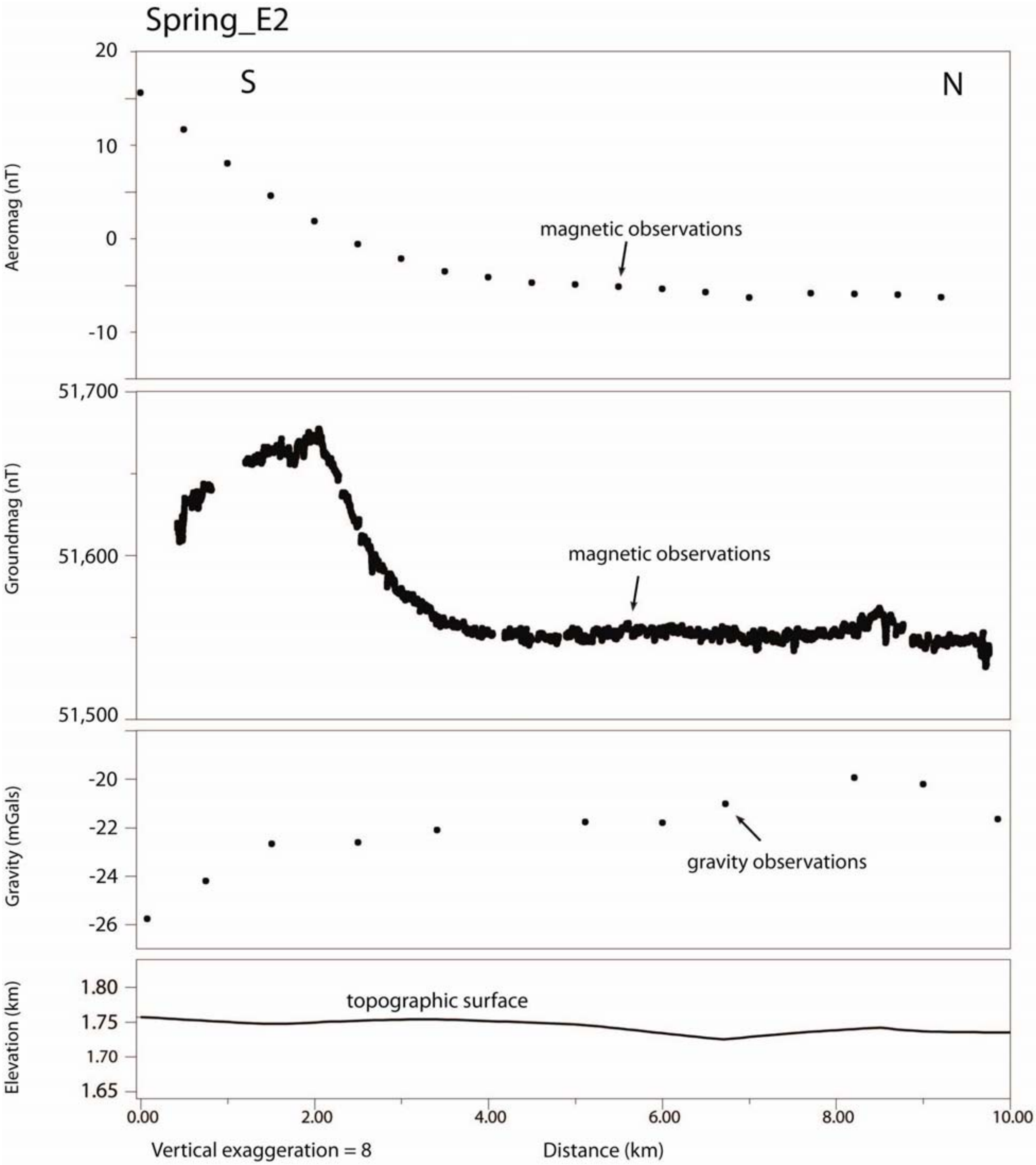

Figure 10. Ground magnetic traverse along line "Spring_E2." Upper panel shows aeromagnetic data from NAMAG (2002) for comparison.

Table 1. Principal facts for new gravity stations, Spring to Delamar Valleys, Nevada

[Station coordinates, NAD27; elevations, NAVD29; Bouguer anomaly calculated using a reduction density of 2670 kg/m³; terrain corrections calculated out to 166.7 km]

Station Name	Longitude °W	Latitude °N	Elevation (meters)	Observed Gravity (mGal)	Free Air Anomaly (mGal)	Total Terrain Correction (mGal)	Complete Bouguer Anomaly (mGal)	Isostatic Anomaly (mGal)
06TIP001	-114.5335	39.7153	1881.5	979541.96	-21.31	1.37	-231.97	-26.53
06TIP002	-114.5023	39.7267	1872.7	979551.79	-15.22	1.11	-225.15	-20.29
06TIP003	-114.4925	39.7308	1898.7	979547.64	-11.70	0.98	-224.69	-20.04
06TIP004	-114.4845	39.7362	1921.2	979543.56	-9.33	0.97	-224.84	-20.42
06TIP005	-114.4753	39.7418	1965.3	979538.23	-1.57	1.15	-221.84	-17.70
06TIP006	-114.4540	39.7443	1880.0	979557.30	-9.01	1.26	-219.62	-15.72
06TIP007	-114.4505	39.7443	1864.1	979559.10	-12.13	1.19	-221.02	-17.16
06TIP008	-114.4437	39.7438	1837.2	979562.80	-16.67	1.09	-222.65	-18.85
06TIP009	-114.4405	39.7437	1827.9	979564.33	-18.00	1.04	-222.98	-19.23
06TIP010	-114.4335	39.7433	1810.8	979566.92	-20.65	0.98	-223.78	-20.12
06TIP011	-114.4305	39.7432	1805.0	979568.16	-21.17	0.95	-223.69	-20.10
06TIP012	-114.4232	39.7427	1796.1	979570.67	-21.37	0.87	-222.96	-19.48
06TIP013	-114.4195	39.7425	1792.1	979572.15	-21.10	0.86	-222.26	-18.82
06TIP014	-114.4680	39.7442	1968.7	979539.92	0.98	1.45	-219.38	-15.38
06TIP015	-114.4117	39.7420	1787.6	979575.83	-18.76	0.80	-219.47	-16.15
06TIP016	-114.4080	39.7418	1787.4	979577.12	-17.54	0.80	-218.22	-14.96
06TIP017	-114.4047	39.7408	1795.0	979576.98	-15.24	0.78	-216.80	-13.59
06TIP018	-114.4017	39.7398	1794.5	979578.96	-13.32	0.78	-214.83	-11.66
06TIP019	-114.3980	39.7398	1800.3	979579.60	-10.90	0.78	-213.05	-9.95
06TIP020	-114.3945	39.7408	1802.6	979581.66	-8.21	0.79	-210.61	-7.59
06TIP021	-114.3875	39.7425	1802.8	979583.42	-6.54	0.85	-208.90	-6.05
06TIP022	-114.3840	39.7418	1799.4	979584.19	-6.77	0.86	-208.73	-5.94
06TIP023	-114.3775	39.7400	1784.2	979588.61	-6.86	0.92	-207.07	-4.38
06TIP024	-114.2900	39.9895	1776.3	979606.93	-13.19	0.88	-212.55	-15.85
06TIP025	-114.2932	39.9898	1784.9	979605.76	-11.74	0.90	-212.05	-15.28
06TIP026	-114.2968	39.9897	1793.0	979604.02	-10.96	0.98	-212.10	-15.25
06TIP027	-114.3007	39.9895	1803.8	979601.27	-10.35	1.07	-212.61	-15.67
06TIP028	-114.3045	39.9893	1820.2	979597.70	-8.85	1.15	-212.86	-15.84
06TIP029	-114.3077	39.9880	1836.6	979593.60	-7.78	1.25	-213.54	-16.44
06TIP030	-114.3117	39.9887	1861.5	979589.55	-4.21	1.36	-212.65	-15.52
06TIP031	-114.3160	39.9883	1882.2	979585.41	-1.94	1.50	-212.55	-15.35
06TIP032	-114.3198	39.9883	1905.0	979580.40	0.07	1.70	-212.89	-15.62
06TIP033	-114.3455	39.8713	1730.7	979595.13	-28.53	2.03	-221.63	-21.32
06TIP034	-114.2860	39.9895	1769.0	979608.47	-13.89	0.82	-212.49	-15.93

06TIP035	-114.2822	39.9897	1764.0	979610.10	-13.81	0.79	-211.89	-15.42
06TIP036	-114.2785	39.9895	1762.4	979611.79	-12.60	0.73	-210.55	-14.16
06TIP037	-114.2745	39.9893	1764.2	979612.07	-11.76	0.71	-209.94	-13.65
06TIP038	-114.2708	39.9902	1769.4	979611.60	-10.70	0.69	-209.48	-13.32
06TIP039	-114.2673	39.9910	1776.5	979610.55	-9.63	0.68	-209.22	-13.17
06TIP040	-114.2637	39.9920	1783.0	979609.46	-8.80	0.65	-209.15	-13.20
06TIP041	-114.2597	39.9930	1792.3	979607.43	-8.06	0.64	-209.46	-13.65
06TIP042	-114.2567	39.9945	1799.9	979607.69	-5.58	0.64	-207.83	-12.14
06TIP043	-114.2537	39.9957	1809.2	979606.68	-3.84	0.64	-207.13	-11.55
06TIP044	-114.2475	39.9973	1825.3	979604.97	-0.73	0.64	-205.82	-10.48
06TIP045	-114.2442	39.9965	1828.9	979603.44	-1.08	0.63	-206.58	-11.31
06TIP046	-114.2407	39.9953	1829.8	979603.38	-0.75	0.62	-206.37	-11.18
06TIP047	-114.2372	39.9945	1833.7	979604.51	1.65	0.63	-204.39	-9.28
06TIP048	-114.2313	39.9937	1835.4	979601.30	-0.95	0.60	-207.22	-12.27
06TIP049	-114.2255	39.9935	1839.2	979600.72	-0.35	0.61	-207.04	-12.26
06TIP050	-114.2937	39.9783	1784.4	979602.29	-14.33	0.94	-214.54	-17.54
06TIP051	-114.3015	39.9540	1779.7	979601.32	-14.59	1.16	-214.06	-16.33
06TIP052	-114.3063	39.9277	1765.0	979597.86	-20.23	1.24	-217.97	-19.61
06TIP053	-114.3173	39.9015	1734.5	979596.73	-28.43	1.45	-222.54	-23.36
06TIP054	-114.3308	39.8868	1720.9	979597.04	-31.01	1.79	-223.25	-23.51
06TIP055	-114.3950	39.7855	1837.9	979577.44	-5.51	1.01	-211.65	-9.24
06TIP056	-114.4098	39.7747	1828.5	979572.83	-12.05	1.08	-217.07	-14.25
06SNW001	-114.5597	38.7943	1829.1	979479.00	-18.80	0.95	-224.02	-19.70
06SNW002	-114.4278	38.6510	1850.9	979470.66	-7.77	0.82	-215.56	-14.47
06SNW003	-114.3763	38.5667	1849.2	979456.68	-14.83	0.48	-222.76	-23.07
06SNW004	-114.3282	38.4667	2042.5	979424.56	21.46	1.47	-207.14	-8.92
06SNW005	-114.4713	38.7243	1809.4	979490.52	-7.17	0.75	-210.38	-7.79
06SNW006	-114.4833	38.7328	1805.7	979490.23	-9.36	0.73	-212.17	-9.35
06SNW007	-114.4922	38.7393	1801.7	979489.77	-11.62	0.72	-214.00	-11.00
06SNW008	-114.5007	38.7460	1792.7	979490.73	-14.04	0.73	-215.39	-12.25
06SNW009	-114.5062	38.7493	1793.0	979490.94	-14.02	0.74	-215.39	-12.16
06SNW010	-114.5162	38.7567	1782.4	979492.21	-16.67	0.78	-216.82	-13.37
06SNW011	-114.5255	38.7635	1779.8	979492.23	-18.06	0.85	-217.84	-14.20
06SNW012	-114.5398	38.7702	1788.6	979488.26	-19.91	0.88	-220.64	-16.86
06SNW013	-114.5450	38.7720	1795.6	979487.08	-19.08	0.88	-220.61	-16.79
06SNW014	-114.5595	38.7743	1823.6	979482.44	-15.30	0.97	-219.87	-15.95
06SNW015	-114.5690	38.7718	1850.0	979477.25	-12.13	1.02	-219.61	-15.74
06SNW016	-114.5737	38.7658	1874.3	979472.75	-8.61	0.86	-218.98	-15.21
06SNW017	-114.5775	38.7693	1887.8	979469.38	-8.13	0.98	-219.88	-16.05
06SNW018	-114.5835	38.7662	1896.1	979467.11	-7.55	0.91	-220.31	-16.54
06SNW019	-114.5947	38.7708	1921.2	979459.70	-7.65	1.01	-223.11	-19.28
06SNW020	-114.6003	38.7658	1910.6	979461.50	-8.67	0.95	-223.01	-19.22
06SNW021	-114.3490	38.5062	1934.8	979442.65	2.86	0.63	-214.51	-15.74
06SNW022	-114.3537	38.5062	1928.0	979444.27	2.40	0.78	-214.07	-15.27
06SNW023	-114.3590	38.5073	1916.2	979445.70	0.08	0.77	-215.08	-16.26
06SNW024	-114.3728	38.5070	1912.2	979445.41	-1.42	0.79	-216.11	-17.31
06SNW025	-114.3772	38.5060	1912.3	979445.06	-1.64	0.86	-216.27	-17.49
06SNW026	-114.3817	38.5052	1923.2	979441.96	-1.31	0.78	-217.24	-18.49

06SNW027	-114.3862	38.5038	1926.0	979441.73	-0.57	0.75	-216.83	-18.14
06SNW028	-114.3903	38.5018	1934.7	979441.06	1.62	0.77	-215.60	-16.95
06SNW029	-114.3927	38.4983	1943.1	979439.61	3.07	0.75	-215.11	-16.53
06SNW030	-114.3943	38.4953	1946.4	979440.92	5.65	0.71	-212.94	-14.39
06SNW031	-114.3973	38.4927	1950.6	979439.42	5.68	0.70	-213.39	-14.88
06SNW032	-114.4057	38.4875	1950.1	979439.55	6.13	0.70	-212.89	-14.49
06SNW033	-114.4120	38.4867	1937.2	979441.98	4.66	0.78	-212.83	-14.43
06SNW034	-114.4167	38.4848	1931.5	979443.76	4.83	0.81	-212.00	-13.65
06SNW035	-114.4200	38.4823	1926.7	979445.94	5.74	0.82	-210.53	-12.20
06SNW036	-114.4237	38.4800	1921.3	979447.38	5.73	0.83	-209.93	-11.65
06SNW037	-114.5545	39.1557	1945.7	979482.02	-11.81	4.68	-226.35	-17.76
06SNW038	-114.5527	39.1553	1935.3	979484.40	-12.60	4.44	-226.22	-17.64
06SNW039	-114.5492	39.1552	1915.3	979487.97	-15.18	3.94	-227.06	-18.49
06SNW040	-114.5475	39.1550	1904.0	979490.09	-16.51	3.73	-227.34	-18.77
06SNW041	-114.5453	39.1548	1895.1	979492.03	-17.31	3.54	-227.33	-18.79
06SNW042	-114.5438	39.1548	1886.6	979493.52	-18.43	3.42	-227.62	-19.08
06SNW043	-114.5423	39.1547	1877.8	979495.11	-19.55	3.31	-227.86	-19.34
06SNW044	-114.5407	39.1547	1867.9	979496.90	-20.82	3.21	-228.11	-19.61
06SNW045	-114.5375	39.1543	1850.4	979499.68	-23.39	3.00	-228.95	-20.47
06SNW046	-114.5355	39.1540	1843.3	979500.78	-24.46	2.85	-229.37	-20.88
06SNW047	-114.5333	39.1537	1833.3	979502.00	-26.28	2.73	-230.19	-21.74
06SNW048	-114.5323	39.1535	1827.9	979502.69	-27.27	2.69	-230.60	-22.16
06SNW049	-114.5303	39.1532	1819.9	979503.41	-28.96	2.60	-231.49	-23.06
06SNW050	-114.5263	39.1527	1810.7	979504.42	-30.74	2.41	-232.44	-24.03
06SNW051	-114.5243	39.1525	1802.7	979504.98	-32.62	2.37	-233.46	-25.08
06SNW052	-114.5223	39.1520	1797.1	979505.36	-33.94	2.29	-234.22	-25.85
06SNW053	-114.5202	39.1518	1792.2	979505.09	-35.71	2.22	-235.52	-27.16
06SNW054	-114.5183	39.1513	1786.4	979504.92	-37.62	2.18	-236.82	-28.47
06SNW055	-114.5168	39.1510	1782.4	979504.56	-39.20	2.11	-238.01	-29.68
06SNW056	-114.5132	39.1480	1772.3	979504.01	-42.58	2.00	-240.38	-32.12
06SNW057	-114.5073	39.1480	1760.9	979502.56	-47.57	1.88	-244.20	-36.02
06SNW058	-114.7047	38.4492	1979.6	979437.34	16.37	1.35	-205.30	-9.36
06SNW059	-114.7155	38.4353	1930.0	979443.46	8.43	1.33	-207.71	-12.18
06SNW060	-114.7203	38.4283	1913.5	979445.07	5.57	1.10	-208.95	-13.61
06SNW061	-114.7260	38.4175	1888.0	979448.56	2.16	0.92	-209.69	-14.67
06SNW062	-114.7207	38.4175	1912.0	979444.87	5.86	0.94	-208.65	-13.61
06SNW063	-114.7152	38.4165	1933.6	979442.29	10.02	1.07	-206.77	-11.75
06SNW064	-114.7095	38.4163	1963.9	979438.78	15.87	1.31	-204.09	-9.06
06SNW065	-114.7045	38.4168	1994.6	979435.58	22.11	1.66	-200.94	-5.90
06SNW066	-114.6997	38.4195	2039.9	979429.67	29.93	2.24	-197.60	-2.52
06SNW067	-114.6955	38.4225	2097.8	979419.57	37.41	3.02	-195.82	-0.67
06SNW068	-114.6963	38.4142	2076.4	979425.86	37.82	2.86	-193.17	1.76
06SNW069	-114.7287	38.4125	1878.4	979449.40	0.46	0.82	-210.41	-15.52
06SNW070	-114.7352	38.3927	1847.7	979450.86	-5.78	0.67	-213.36	-19.09
06SNW071	-114.7417	38.3788	1824.1	979452.17	-10.54	0.62	-215.52	-21.70
06SNW072	-114.7498	38.3625	1796.5	979454.69	-15.10	0.61	-217.00	-23.72
06SNW073	-114.7547	38.3443	1767.4	979459.63	-17.54	0.67	-216.11	-23.31
06SNW074	-114.7500	38.3445	1779.9	979458.05	-15.27	0.59	-215.32	-22.48

06SNW075	-114.7455	38.3452	1792.0	979456.55	-13.08	0.59	-214.49	-21.61
06SNW076	-114.7410	38.3448	1803.8	979455.69	-10.28	0.64	-212.97	-20.07
06SNW077	-114.7363	38.3448	1817.9	979455.20	-6.44	0.69	-210.65	-17.73
06SNW078	-114.7272	38.3445	1860.4	979451.43	2.94	0.85	-205.88	-12.89
06SNW079	-114.7227	38.3443	1887.2	979449.80	9.58	0.98	-202.12	-9.13
06SNW080	-114.7178	38.3450	1914.4	979447.68	15.80	1.14	-198.79	-5.78
06SNW081	-114.7058	38.3472	1992.3	979436.19	28.13	1.77	-194.54	-1.43
06SNW082	-114.7003	38.3485	2035.2	979426.93	31.97	2.26	-195.01	-1.85
06SNW083	-114.6948	38.3500	2096.0	979414.39	38.05	2.94	-195.06	-1.88
06SNW084	-114.6890	38.3492	2164.5	979400.31	45.15	4.14	-194.41	-1.28
06SNW085	-114.7565	38.3355	1763.1	979460.20	-17.51	0.60	-215.67	-23.15
06SNW086	-114.7112	38.3115	1857.0	979447.87	1.23	0.95	-207.11	-14.91
06SNW087	-114.6982	38.3050	1880.7	979450.92	12.16	0.93	-198.85	-6.73
06SNW088	-114.6850	38.2957	1936.4	979437.95	17.18	1.14	-199.86	-7.95
06SNW089	-114.6963	38.2803	1891.7	979442.47	9.27	0.68	-203.23	-11.83
06SNW090	-114.7092	38.2708	1848.4	979444.68	-1.02	0.57	-208.79	-17.81
06SNW091	-114.7120	38.2635	1843.2	979446.15	-0.52	0.51	-207.75	-17.00
06SNW092	-114.7177	38.2598	1826.4	979444.98	-6.54	0.48	-211.93	-21.33
06SNW093	-114.7223	38.2627	1819.4	979444.34	-9.59	0.46	-214.21	-23.59
06SNW094	-114.7260	38.2662	1810.4	979445.13	-11.88	0.45	-215.50	-24.82
06SNW095	-114.7343	38.2740	1788.9	979447.79	-16.54	0.43	-217.77	-26.92
06SNW096	-114.7402	38.2783	1773.1	979450.70	-18.88	0.45	-218.32	-27.39
06SNW097	-114.7527	38.2812	1755.7	979453.57	-21.64	0.40	-219.17	-28.24
06SNW098	-114.7578	38.2830	1737.7	979457.19	-23.72	0.45	-219.19	-28.25
06SNW099	-114.7635	38.2842	1727.7	979459.75	-24.36	0.46	-218.70	-27.81
06SNW100	-114.7695	38.2842	1715.6	979462.46	-25.37	0.49	-218.32	-27.47
06SNW101	-114.7818	38.2860	1722.5	979463.38	-22.50	0.53	-216.18	-25.42
06SNW102	-114.7872	38.2870	1731.4	979463.15	-20.06	0.57	-214.70	-24.00
06SNW103	-114.7918	38.2875	1744.6	979461.32	-17.87	0.56	-214.00	-23.31
06SNW104	-114.7962	38.2887	1757.6	979459.71	-15.58	0.59	-213.13	-22.46
06SNW105	-114.8005	38.2898	1768.1	979458.29	-13.84	0.67	-212.50	-21.84
06SNW106	-114.8048	38.2910	1787.6	979455.69	-10.54	0.70	-211.35	-20.73
06SNW107	-114.8092	38.2920	1798.5	979454.38	-8.57	0.81	-210.50	-19.94
06SNW108	-114.8137	38.2930	1815.1	979453.02	-4.92	0.94	-208.57	-18.06
06SNW109	-114.8183	38.2930	1836.8	979453.70	2.46	1.03	-203.54	-13.11
06SNW110	-114.8225	38.2943	1858.6	979453.07	8.45	1.20	-199.82	-9.38
06SNW111	-114.8273	38.2948	1869.0	979454.36	12.88	1.40	-196.35	-5.96
06SNW112	-114.8310	38.2975	1892.1	979452.35	17.78	1.84	-193.61	-3.23
06SNW113	-114.8345	38.3002	1926.9	979446.25	22.18	2.10	-192.85	-2.46
06SNW114	-114.8175	38.2858	1811.0	979454.68	-3.88	0.79	-207.23	-16.98
06SNW115	-114.8147	38.2807	1786.2	979457.30	-8.46	0.67	-209.15	-19.01
06SNW116	-114.8095	38.2705	1739.8	979463.16	-16.00	0.55	-211.60	-21.67
06SNW117	-114.8063	38.2657	1722.2	979465.48	-18.70	0.50	-212.37	-22.53
06SNW118	-114.8033	38.2608	1704.7	979467.00	-22.15	0.48	-213.88	-24.14
06SNW119	-114.8003	38.2560	1690.5	979468.34	-24.75	0.46	-214.91	-25.25
06SNW120	-114.8047	38.2440	1665.9	979474.16	-25.47	0.51	-212.82	-23.55
06SNW121	-114.8138	38.2367	1669.3	979474.00	-23.93	0.50	-211.68	-22.78
06SNW122	-114.8203	38.2357	1678.7	979472.72	-22.22	0.52	-211.00	-22.22

06SNW123	-114.8317	38.2332	1703.2	979470.25	-16.92	0.59	-208.38	-19.82
06SNW124	-114.8372	38.2322	1718.6	979469.02	-13.33	0.63	-206.47	-18.02
06SNW125	-114.8430	38.2308	1734.4	979467.83	-9.51	0.71	-204.35	-16.01
06SNW126	-114.8485	38.2295	1751.3	979466.28	-5.75	0.80	-202.38	-14.16
06SNW127	-114.8538	38.2285	1770.3	979464.56	-1.53	0.96	-200.13	-12.02
06SNW128	-114.6492	38.2685	2060.8	979407.10	27.06	1.36	-203.68	-12.32
06SNW129	-114.6625	38.2675	1978.4	979424.15	18.80	1.00	-203.08	-11.75
06SNW130	-114.6698	38.2667	1945.7	979428.70	13.36	0.86	-205.01	-13.78
06SNW131	-114.6817	38.2617	1909.3	979434.06	7.93	0.85	-206.37	-15.39
06SNW132	-114.6882	38.2578	1891.8	979436.76	5.58	0.78	-206.83	-16.01
06SNW133	-114.6970	38.2568	1867.4	979441.46	2.83	0.71	-206.91	-16.21
06SNW134	-114.7095	38.2532	1839.3	979446.97	0.01	0.54	-206.75	-16.27
06SNW135	-114.7152	38.2525	1824.2	979446.84	-4.72	0.53	-209.80	-19.39
06SNW136	-114.7210	38.2522	1812.6	979447.23	-7.88	0.48	-211.71	-21.39
06SNW137	-114.7265	38.2510	1800.2	979448.00	-10.82	0.47	-213.28	-23.03
06SNW138	-114.7322	38.2502	1788.9	979449.45	-12.78	0.44	-214.00	-23.84
06SNW139	-114.7378	38.2485	1782.0	979450.23	-14.00	0.41	-214.47	-24.41
06SNW140	-114.7492	38.2478	1760.8	979453.28	-17.41	0.38	-215.54	-25.62
06SNW141	-114.7547	38.2473	1751.5	979455.04	-18.47	0.36	-215.58	-25.73
06SNW142	-114.7603	38.2470	1737.4	979457.62	-20.23	0.37	-215.74	-25.97
06SNW143	-114.7662	38.2468	1731.1	979459.19	-20.58	0.34	-215.42	-25.73
06SNW144	-114.7773	38.2453	1711.2	979463.92	-21.84	0.34	-214.45	-24.89
06SNW145	-114.7830	38.2443	1701.2	979465.85	-22.91	0.36	-214.38	-24.93
06SNW146	-114.7888	38.2440	1690.4	979468.18	-23.90	0.38	-214.13	-24.73
06SNW147	-114.7967	38.2425	1675.1	979471.66	-24.99	0.45	-213.44	-24.12
06SNW148	-114.7955	38.2490	1671.3	979472.19	-26.22	0.49	-214.19	-24.67
06SNW149	-114.7877	38.2665	1688.2	979469.22	-25.51	0.52	-215.36	-25.22
06SNW150	-114.7787	38.2783	1697.4	979466.15	-26.77	0.58	-217.59	-26.99
06SNW151	-114.7557	38.2945	1747.1	979457.52	-21.50	0.45	-218.03	-26.71
06SNW152	-114.7485	38.2885	1760.5	979453.95	-20.42	0.44	-218.45	-27.24
06SNW153	-114.7448	38.2635	1773.2	979449.88	-18.37	0.39	-217.88	-27.48
06SNW154	-114.7462	38.2422	1762.0	979454.17	-15.68	0.40	-213.91	-24.12
06SNW155	-114.7458	38.2358	1760.0	979455.90	-13.98	0.42	-211.98	-22.38
06SNW156	-114.7452	38.2295	1767.2	979454.39	-12.73	0.42	-211.54	-22.16
06SNW157	-114.7423	38.2233	1778.2	979453.95	-9.22	0.46	-209.23	-20.09
06SNW158	-114.7390	38.2123	1789.1	979455.37	-3.48	0.52	-204.64	-15.78
06SNW159	-114.7392	38.2065	1776.4	979460.39	-1.87	0.61	-201.51	-12.83
06SNW160	-114.7358	38.1977	1795.5	979459.35	3.76	0.68	-197.96	-9.54
06SNW161	-114.7348	38.1917	1800.1	979460.82	7.17	0.68	-195.06	-6.82
06SNW162	-114.7337	38.1862	1805.3	979459.82	8.26	0.72	-194.51	-6.45
06SNW163	-114.7327	38.1805	1813.2	979459.98	11.34	0.73	-192.30	-4.44
06SNW164	-114.7203	38.1800	1852.5	979452.85	16.37	1.03	-191.37	-3.39
06SNW165	-114.7145	38.1853	1889.8	979441.45	16.03	0.94	-196.00	-7.81
06SNW166	-114.7112	38.1905	1920.8	979434.32	18.00	1.01	-197.43	-9.05
06SNW167	-114.7075	38.1997	1900.2	979435.90	12.40	0.99	-200.73	-11.99
06SNW168	-114.7088	38.2065	1866.9	979441.54	7.18	0.92	-202.29	-13.32
06SNW169	-114.7085	38.2135	1873.6	979440.03	7.12	0.85	-203.17	-13.96
06SNW170	-114.7042	38.2243	1877.3	979440.17	7.45	0.84	-203.28	-13.70

06SNW171	-114.7027	38.2380	1854.8	979443.34	2.50	0.72	-205.83	-15.74
06SNW172	-114.7095	38.3170	1882.6	979446.54	7.32	1.23	-203.61	-11.28
06SNW173	-114.7077	38.3217	1901.8	979445.47	11.74	1.55	-201.01	-8.57
06SNW174	-114.7065	38.3308	1939.5	979440.04	17.15	1.54	-199.85	-7.17
06SNW175	-114.6930	38.3448	2100.1	979411.73	37.13	3.25	-196.13	-3.07
06SNW176	-114.6980	38.3427	2037.7	979422.87	29.22	2.46	-197.86	-4.82
06SNW177	-114.7035	38.3408	1990.1	979432.05	23.88	1.87	-198.45	-5.46
06SNW178	-114.7098	38.3408	1940.2	979442.50	18.94	1.45	-198.22	-5.27
06SNW179	-114.7620	38.3443	1770.3	979460.33	-15.92	0.63	-214.86	-22.16
06SNW180	-114.7645	38.3483	1781.7	979459.48	-13.59	0.56	-213.89	-21.12
06SNW181	-114.7667	38.3565	1794.4	979458.70	-11.19	0.57	-212.90	-19.95
06SNW182	-114.7673	38.3612	1801.5	979458.21	-9.91	0.58	-212.41	-19.35
06SNW183	-114.7698	38.3657	1812.3	979458.73	-6.44	0.54	-210.19	-17.01
06SNW184	-114.7732	38.3738	1833.6	979458.14	-1.21	0.51	-207.36	-14.01
06SNW185	-114.7743	38.3823	1843.4	979457.73	0.66	0.54	-206.56	-12.95
06SNW186	-114.7742	38.3878	1856.6	979456.70	3.22	0.54	-205.49	-11.76
06SNW187	-114.7757	38.3927	1870.0	979454.96	5.18	0.57	-204.99	-11.11
06SNW188	-114.7780	38.4055	1904.6	979450.30	10.06	0.80	-203.77	-9.62
06SNW189	-114.7778	38.4013	1890.7	979452.51	8.37	0.72	-203.98	-9.92
06SNW190	-114.7732	38.4028	1896.0	979451.01	8.37	0.66	-204.63	-10.49
06SNW191	-114.7683	38.4055	1903.3	979449.16	8.53	0.65	-205.30	-11.05
06SNW192	-114.7625	38.4042	1896.9	979449.36	6.86	0.63	-206.27	-12.00
06SNW193	-114.7555	38.4085	1885.3	979451.98	5.55	0.74	-206.17	-11.68
06SNW194	-114.7537	38.4128	1909.9	979449.08	9.82	0.76	-204.64	-10.08
06SNW195	-114.7465	38.4133	1898.6	979449.11	6.34	0.71	-206.90	-12.25
06SNW196	-114.7410	38.4165	1907.2	979447.57	7.17	0.78	-206.97	-12.17
06SNW197	-114.7368	38.4218	1919.5	979445.44	8.35	0.88	-207.06	-12.12
06SNW198	-114.7270	38.4317	1915.5	979446.51	7.33	1.16	-207.35	-11.99
06SNW199	-114.7210	38.4387	1941.3	979442.23	10.40	1.29	-207.04	-11.46
06SNW200	-114.5633	39.0493	1868.2	979484.43	-23.88	2.17	-232.25	-24.30
06SNW201	-114.5610	39.0495	1859.2	979485.92	-25.18	2.05	-232.65	-24.72
06SNW202	-114.5588	39.0502	1850.6	979487.57	-26.24	2.00	-232.81	-24.87
06SNW203	-114.5573	39.0477	1852.1	979486.37	-26.75	1.84	-233.65	-25.77
06SNW204	-114.5555	39.0465	1850.2	979486.22	-27.37	1.73	-234.17	-26.32
06SNW205	-114.5535	39.0455	1845.1	979485.96	-29.11	1.68	-235.39	-27.57
06SNW206	-114.5513	39.0448	1844.2	979485.34	-29.95	1.59	-236.22	-28.44
06SNW207	-114.5495	39.0458	1839.0	979486.55	-30.42	1.55	-236.15	-28.38
06SNW208	-114.5467	39.0468	1829.0	979487.65	-32.50	1.53	-237.13	-29.35
06SNW209	-114.5623	39.0838	1933.4	979478.40	-12.83	2.22	-228.47	-20.32
06SNW210	-114.5597	39.0848	1909.9	979482.27	-16.31	2.12	-229.41	-21.25
06SNW211	-114.5568	39.0848	1892.6	979484.23	-19.68	2.01	-230.95	-22.80
06SNW212	-114.5547	39.0835	1880.8	979485.83	-21.60	1.96	-231.60	-23.47
06SNW213	-114.5525	39.0835	1878.7	979486.16	-21.91	1.82	-231.81	-23.69
06SNW214	-114.5498	39.0833	1874.8	979485.75	-23.51	1.73	-233.07	-25.00
06SNW215	-114.5473	39.0837	1870.7	979485.81	-24.75	1.66	-233.92	-25.85
06SNW216	-114.5452	39.0838	1865.3	979486.07	-26.16	1.62	-234.76	-26.71
06SNW217	-114.5432	39.0825	1857.2	979486.78	-27.86	1.59	-235.57	-27.55
06SNW218	-114.5415	39.0813	1852.8	979486.90	-28.98	1.55	-236.24	-28.24

06SNW219	-114.5397	39.0802	1845.2	979487.65	-30.46	1.54	-236.89	-28.91
06SNW220	-114.5378	39.0790	1839.0	979487.94	-31.97	1.52	-237.72	-29.76
06SNW221	-114.5447	39.2135	1919.0	979488.13	-19.03	4.45	-230.82	-22.08
06SNW222	-114.5425	39.2133	1913.5	979489.15	-19.70	4.17	-231.15	-22.41
06SNW223	-114.5393	39.2133	1904.3	979490.87	-20.81	3.91	-231.48	-22.79
06SNW224	-114.5313	39.2098	1882.2	979494.61	-23.59	3.25	-232.45	-23.88
06SNW225	-114.5222	39.2095	1856.8	979499.31	-26.67	2.86	-233.08	-24.59
06SNW226	-114.5133	39.2078	1835.0	979503.13	-29.45	2.51	-233.76	-25.34
06SNW227	-114.5112	39.2075	1829.2	979504.15	-30.17	2.45	-233.89	-25.50
06SNW228	-114.5035	39.2062	1810.2	979507.25	-32.80	2.25	-234.60	-26.28
06SNW229	-114.5408	38.8560	1830.4	979482.05	-20.81	1.18	-225.93	-20.63
06SNW230	-114.5452	38.8572	1836.0	979482.31	-18.93	1.27	-224.59	-19.25
06SNW231	-114.5490	38.8595	1846.1	979480.60	-17.73	1.36	-224.43	-19.05
06SNW232	-114.5535	38.8603	1859.6	979477.17	-17.06	1.37	-225.27	-19.86
06SNW233	-114.5582	38.8612	1871.7	979474.09	-16.49	1.46	-225.97	-20.56
06SNW234	-114.5623	38.8628	1889.3	979469.85	-15.45	1.52	-226.84	-21.39
06SNW235	-114.5663	38.8645	1907.5	979465.94	-13.88	1.61	-227.22	-21.73
06SNW236	-114.5782	38.8682	1961.2	979456.48	-7.12	1.99	-226.09	-20.54
06SNW237	-114.5833	38.8708	1987.1	979451.82	-4.03	2.26	-225.63	-20.07
06SNW238	-114.5913	38.8783	2046.0	979441.75	3.39	2.96	-224.10	-18.46
06SNW239	-114.5973	38.8798	2082.9	979434.23	7.12	3.82	-223.64	-18.04
06SNW240	-114.5325	38.8528	1813.2	979481.51	-26.36	1.08	-229.66	-24.46
06SNW241	-114.5275	38.8513	1804.0	979483.11	-27.48	1.03	-229.79	-24.59
06SNW242	-114.5213	38.8515	1793.1	979484.96	-29.01	1.01	-230.13	-24.96
06SNW243	-114.5103	38.8513	1774.6	979488.05	-31.58	0.99	-230.65	-25.53
06SNW244	-114.3563	38.7948	1906.3	979467.40	-6.64	6.26	-215.19	-12.41
06SNW245	-114.3610	38.7957	1874.5	979471.50	-12.44	5.06	-218.62	-15.71
06SNW246	-114.3652	38.7972	1847.8	979476.63	-15.66	4.48	-219.43	-16.41
06SNW247	-114.3693	38.7985	1833.6	979479.72	-17.08	3.93	-219.81	-16.70
06SNW248	-114.3740	38.7993	1815.6	979483.03	-19.38	3.45	-220.58	-17.36
06SNW249	-114.3787	38.7998	1802.1	979485.31	-21.31	3.05	-221.39	-18.14
06SNW250	-114.3832	38.8005	1787.8	979488.01	-23.08	2.75	-221.86	-18.54
06SNW251	-114.3882	38.8013	1776.2	979490.76	-23.97	2.46	-221.74	-18.36
06SNW252	-114.3412	38.7330	1956.8	979461.72	8.69	2.04	-209.73	-8.00
06SNW253	-114.3433	38.7332	1947.2	979461.98	6.01	1.96	-211.42	-9.68
06SNW254	-114.3457	38.7337	1936.2	979462.90	3.48	1.93	-212.75	-10.99
06SNW255	-114.3478	38.7342	1924.9	979464.82	1.87	1.90	-213.12	-11.31
06SNW256	-114.3500	38.7347	1917.8	979466.29	1.10	1.84	-213.15	-11.30
06SNW257	-114.3522	38.7353	1909.2	979468.15	0.26	1.82	-213.06	-11.18
06SNW258	-114.3545	38.7358	1899.5	979469.97	-0.95	1.76	-213.24	-11.30
06SNW259	-114.3567	38.7363	1891.3	979471.53	-1.98	1.72	-213.39	-11.43
06SNW260	-114.3588	38.7370	1881.8	979473.35	-3.14	1.69	-213.52	-11.51
06SNW261	-114.3612	38.7373	1873.2	979475.02	-4.16	1.63	-213.63	-11.59
06SNW262	-114.3633	38.7382	1865.3	979476.40	-5.30	1.59	-213.92	-11.82
06SNW263	-114.4245	38.5893	1943.9	979444.19	-0.13	1.88	-217.27	-17.31
06SNW264	-114.4222	38.5893	1925.5	979446.93	-3.07	1.44	-218.59	-18.60
06SNW265	-114.4198	38.5895	1920.8	979446.26	-5.19	1.20	-220.42	-20.44
06SNW266	-114.4175	38.5895	1911.0	979447.33	-7.13	1.09	-221.39	-21.41

06SNW267	-114.4152	38.5895	1900.1	979449.60	-8.24	1.01	-221.34	-21.34
06SNW268	-114.4130	38.5895	1893.3	979451.44	-8.49	0.94	-220.91	-20.90
06SNW269	-114.4107	38.5895	1888.8	979452.98	-8.32	0.86	-220.31	-20.31
06SNW270	-114.4085	38.5897	1882.5	979454.45	-8.83	0.81	-220.16	-20.15
06SNW271	-114.4062	38.5897	1874.6	979455.95	-9.77	0.78	-220.25	-20.24
06SNW272	-114.4038	38.5897	1868.4	979457.13	-10.50	0.73	-220.33	-20.32
06SNW273	-114.4015	38.5897	1863.3	979457.82	-11.37	0.69	-220.67	-20.66
06SNW274	-114.3970	38.5898	1854.7	979459.19	-12.69	0.62	-221.09	-21.07
06SNW275	-114.3947	38.5898	1850.0	979459.73	-13.57	0.60	-221.47	-21.45
06SNW276	-114.3815	38.5900	1834.8	979460.11	-17.90	0.48	-224.22	-24.18
06SNW277	-114.6963	38.3927	2006.3	979439.39	31.64	1.82	-192.55	1.93
06SNW278	-114.7058	38.3955	1969.9	979441.23	22.02	1.24	-198.68	-4.19
06SNW279	-114.7102	38.3942	1940.7	979444.59	16.47	1.09	-201.09	-6.64
06SNW280	-114.7145	38.3928	1921.0	979446.26	12.21	0.93	-203.32	-8.93
06SNW281	-114.7187	38.3917	1900.5	979447.89	7.61	0.84	-205.72	-11.35
06SNW282	-114.7230	38.3903	1886.5	979448.66	4.18	0.77	-207.65	-13.36
06SNW283	-114.7273	38.3892	1875.5	979449.33	1.57	0.71	-209.08	-14.86
06SNW284	-114.7317	38.3878	1860.3	979450.10	-2.24	0.67	-211.23	-17.07
06SNW285	-114.7360	38.3867	1849.2	979449.95	-5.72	0.64	-213.49	-19.42
06SNW286	-114.7035	38.3615	2005.8	979435.19	30.04	1.98	-193.93	-0.42
06SNW287	-114.7170	38.3640	1918.1	979446.07	13.66	1.13	-201.35	-7.80
06SNW288	-114.7238	38.3647	1879.0	979449.92	5.39	0.92	-205.45	-11.89
06SNW289	-114.7297	38.3662	1853.7	979451.46	-1.01	0.78	-209.15	-15.57
06SNW290	-114.7642	38.3345	1769.0	979461.61	-14.18	0.60	-213.01	-20.64
06SNW291	-114.7717	38.3325	1790.8	979459.90	-9.00	0.65	-210.22	-17.98
06SNW292	-114.7890	38.3238	1860.2	979447.46	0.73	0.99	-207.93	-16.28
06SNW293	-114.7917	38.3137	1827.3	979450.83	-5.16	0.88	-210.24	-18.84
06SNW294	-114.8025	38.2982	1806.5	979453.11	-7.94	0.79	-210.77	-19.95
06SNW295	-114.8150	38.2672	1743.4	979463.61	-14.16	0.57	-210.15	-20.36
06SNW296	-114.8175	38.2587	1721.2	979467.62	-16.23	0.56	-209.74	-20.22
06SNW297	-114.8300	38.2238	1691.0	979472.61	-17.49	0.56	-207.62	-19.35
06SNW298	-114.6692	38.3178	1982.8	979431.91	23.50	1.63	-198.25	-5.55
06SNW299	-114.6813	38.3087	1927.1	979442.47	17.69	1.23	-198.22	-5.87
06SNW300	-114.7098	38.3047	1856.4	979447.14	0.92	0.75	-207.55	-15.52
06SNW301	-114.7178	38.3060	1835.3	979447.68	-5.17	0.66	-211.37	-19.41
06SNW302	-114.7248	38.3055	1815.8	979449.06	-9.76	0.57	-213.86	-21.96
06SNW303	-114.7522	38.3018	1759.7	979456.14	-19.66	0.46	-217.58	-26.03
06SNW304	-114.7630	38.3022	1729.0	979462.50	-22.80	0.55	-217.18	-25.71
06SNW305	-114.7632	38.3098	1733.6	979463.31	-21.23	0.58	-216.10	-24.40
06SNW306	-114.7567	38.3120	1745.7	979460.87	-20.14	0.54	-216.41	-24.60
06SNW307	-114.7490	38.3125	1757.0	979458.55	-19.01	0.55	-216.55	-24.69
06SNW308	-114.7413	38.3160	1773.9	979456.26	-16.40	0.58	-215.80	-23.75
06SNW309	-114.7350	38.3195	1798.6	979453.33	-12.01	0.60	-214.16	-21.95
06SNW310	-114.7252	38.3197	1821.9	979451.58	-6.60	0.74	-211.21	-18.89
06SNW311	-114.7380	38.3265	1800.8	979453.31	-11.97	0.61	-214.36	-21.99
06SNW312	-114.7505	38.3327	1771.7	979457.61	-17.19	0.59	-216.33	-23.85
06SNW313	-114.7730	38.3532	1792.0	979461.40	-8.95	0.63	-210.32	-17.50
06SNW314	-114.7815	38.3627	1808.4	979464.17	-1.94	0.76	-205.03	-12.07

06SNW315	-114.8083	38.2848	1785.2	979456.29	-10.14	0.65	-210.73	-20.34
06SNW316	-114.8340	38.2507	1733.6	979467.79	-11.54	0.72	-206.28	-17.21
06SNW317	-114.8367	38.2100	1681.7	979475.63	-16.14	0.65	-205.13	-17.35
06SNW318	-114.8413	38.1975	1683.2	979478.96	-11.24	0.66	-200.38	-13.02
06SNW319	-114.8432	38.1903	1671.2	979482.33	-10.96	0.65	-198.77	-11.66
06SNW320	-114.8480	38.1785	1657.5	979485.98	-10.48	0.62	-196.78	-10.12
06SNW321	-114.8515	38.1730	1653.7	979485.73	-11.40	0.59	-197.31	-10.87
06SNW322	-114.8610	38.1683	1668.9	979483.15	-8.91	0.61	-196.50	-10.30
06SNW323	-114.8453	38.1692	1631.2	979488.94	-14.82	0.53	-198.26	-11.88
06SNW324	-114.8400	38.1673	1616.0	979493.16	-15.12	0.52	-196.86	-10.44
06SNW325	-114.8345	38.1647	1600.0	979496.30	-16.68	0.52	-196.63	-10.20
06SNW326	-114.8287	38.1742	1601.5	979493.43	-19.91	0.54	-200.01	-13.25
06SNW327	-114.8233	38.1890	1614.3	979487.63	-23.08	0.56	-204.59	-17.30
06SNW328	-114.8190	38.2017	1625.1	979487.73	-20.74	0.56	-203.46	-15.69
06SNW329	-114.6803	38.2438	1913.6	979428.11	4.86	1.22	-209.54	-19.09
06SNW330	-114.6878	38.2467	1890.8	979434.73	4.21	1.01	-207.85	-17.36
06SNW331	-114.6953	38.2473	1877.9	979439.29	4.74	0.70	-206.19	-15.75
06SNW332	-114.6997	38.2295	1886.6	979437.29	7.00	1.04	-204.57	-14.79
06SNW333	-114.7272	38.1690	1836.3	979453.23	12.75	0.82	-193.40	-5.89
06SNW334	-114.7268	38.1550	1795.6	979459.72	7.91	0.96	-193.53	-6.40
06SNW335	-114.7033	38.0975	1633.5	979485.32	-11.42	0.65	-195.00	-9.25
06SNW336	-114.7190	38.0918	1595.6	979498.72	-9.21	0.84	-188.35	-2.98
06SNW337	-114.7332	38.0890	1583.5	979500.10	-11.33	0.59	-189.35	-4.26
06SNW338	-114.7405	38.0852	1570.9	979496.79	-18.17	0.49	-194.89	-9.97
06SNW339	-114.7687	38.0720	1527.5	979497.14	-30.05	0.34	-202.04	-17.94
06SNW340	-114.7525	38.0793	1549.1	979494.71	-26.45	0.40	-200.81	-16.26
06SNW341	-114.7502	38.1583	1730.7	979466.67	-5.44	0.52	-200.05	-13.03
06SNW342	-114.7650	38.1708	1718.6	979473.09	-3.84	0.46	-197.16	-9.91
06SNW343	-114.7943	38.1920	1656.5	979485.26	-12.70	0.39	-199.12	-11.41
06SNW344	-114.8055	38.1998	1641.2	979485.34	-18.01	0.43	-202.67	-14.82
06SNW345	-114.8115	38.2042	1635.6	979485.52	-19.95	0.48	-203.94	-16.02
06SNW346	-114.8265	38.2122	1656.5	979478.23	-21.49	0.57	-207.73	-19.75
06SNW347	-114.8418	38.2198	1707.5	979472.56	-12.11	0.75	-203.89	-15.89
06SNW348	-114.8662	38.2312	1833.3	979458.15	11.28	1.29	-194.06	-6.07
06SNW349	-115.0143	38.8035	1704.4	979499.02	-38.03	1.76	-228.46	-25.53
06SNW350	-115.0267	38.8027	1670.0	979498.43	-49.17	1.42	-236.07	-33.24
06SNW351	-115.0322	38.8085	1667.1	979498.72	-50.30	1.23	-237.06	-34.15
06SNW352	-115.0407	38.7878	1659.7	979496.73	-52.73	1.15	-238.75	-36.46
06SNW353	-115.0147	38.7893	1686.5	979500.22	-41.13	2.07	-229.23	-26.62
06SNW354	-115.0412	38.7593	1674.6	979496.45	-45.89	1.23	-233.50	-31.99
06SNW355	-115.0552	38.7483	1663.9	979497.61	-47.08	1.02	-233.70	-32.67
06SNW356	-115.0688	38.7375	1649.6	979499.92	-48.23	0.86	-233.39	-32.73
06SNW357	-115.0195	38.8407	1689.4	979503.89	-41.10	1.34	-230.25	-26.42
06SNW358	-115.0263	38.8303	1677.4	979502.81	-44.96	1.25	-232.86	-29.36
06SNW359	-115.0323	38.8210	1667.3	979501.48	-48.56	1.18	-235.41	-32.23
06SNW360	-115.0137	38.8267	1711.5	979503.30	-33.62	1.51	-225.08	-21.57
06SNW361	-115.0050	38.8363	1746.8	979498.98	-27.91	1.61	-223.23	-19.47
06SNW362	-114.9838	38.8357	1837.8	979486.96	-11.83	2.23	-216.73	-12.84

06SNW363	-114.9953	38.8208	1771.9	979494.98	-22.79	2.15	-220.40	-16.97
06SNW364	-115.0013	38.8062	1750.9	979496.80	-26.16	2.25	-221.31	-18.24
06SNW365	-115.0050	38.7933	1714.8	979500.40	-32.56	2.54	-223.36	-20.63
06SNW366	-115.0037	38.7757	1722.5	979501.29	-27.75	3.21	-218.74	-16.48
06SNW367	-115.0118	38.7537	1727.6	979499.19	-26.32	2.58	-218.53	-16.89
06SNW368	-115.0273	38.7420	1725.0	979495.37	-29.91	1.71	-222.69	-21.50
06SNW369	-115.0748	38.6745	1634.6	979502.53	-44.68	1.18	-227.85	-29.01
06SNW370	-115.0877	38.6732	1623.7	979498.97	-51.48	0.86	-233.75	-35.12
06SNW371	-115.0830	38.6918	1623.6	979503.84	-48.27	0.96	-230.43	-31.17
06SNW372	-115.0827	38.7083	1630.2	979501.76	-49.77	0.85	-232.79	-33.11
06SNW373	-115.0370	38.5827	1663.2	979485.63	-44.64	1.05	-231.16	-34.52
06SNW374	-115.0615	38.6612	1687.4	979502.89	-26.85	1.62	-215.51	-16.96
06SNW375	-115.0517	38.6725	1734.1	979499.34	-16.99	2.32	-210.19	-11.30
06SNW376	-115.0153	38.7722	1687.8	979498.11	-41.31	2.26	-229.36	-27.25
06SNW377	-115.0047	38.8465	1714.4	979506.30	-31.49	1.77	-223.02	-19.00
06SNW378	-114.9795	38.8793	1784.5	979493.12	-25.96	2.45	-224.67	-19.69

Table 2. Cenozoic density-depth function for the Spring to Delamar Valleys study area.

Depth Range (km)	**Sedimentary rocks (kg/m^3)**	**Volcanic rocks (kg/m^3)**
0 to 0.2	2020	2220
0.2 to 0.6	2120	2270
0.6 to 1.2	2320	2320
> 1.2	2420	2420